AD

TECHNICAL REPORT ARBRL-TR-02563

CONTRIBUTION OF PRESSURE TO THE MOMENT DURING SPIN-UP ON A NUTATING LIQUID-FILLED CYLINDER: AD HOC MODEL

Nathan Gerber

June 1984

US ARMY ARMAMENT RESEARCH AND DEVELOPMENT CENTER
BALLISTIC RESEARCH LABORATORY
ABERDEEN PROVING GROUND, MARYLAND

Destroy this report when it is no longer needed.
Do not return it to the originator.

Additional copies of this report may be obtained from the National Technical Information Service, U. S. Department of Commerce, Springfield, Virginia 22161.

The findings in this report are not to be construed as an official Department of the Army position, unless so designated by other authorized documents.

The use of trade names or manufacturers' names in this report does not constitute indorsement of any commercial product.

UNCLASSIFIED

SECURITY CLASSIFICATION OF THIS PAGE (When Data Entered)

REPORT DOCUMENTATION PAGE		READ INSTRUCTIONS BEFORE COMPLETING FORM
1. REPORT NUMBER TECHNICAL REPORT ARBRL-TR-02563	2. GOVT ACCESSION NO.	3. RECIPIENT'S CATALOG NUMBER
4. TITLE (and Subtitle) CONTRIBUTION OF PRESSURE TO THE MOMENT DURING SPIN-UP ON A NUTATING LIQUID-FILLED CYLINDER: AD HOC MODEL		5. TYPE OF REPORT & PERIOD COVERED Final 6. PERFORMING ORG. REPORT NUMBER
7. AUTHOR(s) Nathan Gerber		8. CONTRACT OR GRANT NUMBER(s)
9. PERFORMING ORGANIZATION NAME AND ADDRESS US Army Ballistic Research Laboratory, ARDC ATTN: DRSMC-BLL(A) Aberdeen Proving Ground, MD 21005		10. PROGRAM ELEMENT, PROJECT, TASK AREA & WORK UNIT NUMBERS RDT&E 1L161102AH43
11. CONTROLLING OFFICE NAME AND ADDRESS US Army AMCCOM, ARDC Ballistic Research Laboratory, ATTN: DRSMC-BLA-S(A) Aberdeen Proving Ground, MD 21005		12. REPORT DATE June 1984 13. NUMBER OF PAGES 55
14. MONITORING AGENCY NAME & ADDRESS(if different from Controlling Office)		15. SECURITY CLASS. (of this report) UNCLASSIFIED 15a. DECLASSIFICATION/DOWNGRADING SCHEDULE

16. DISTRIBUTION STATEMENT (of this Report)

Approved for public release; distribution unlimited.

17. DISTRIBUTION STATEMENT (of the abstract entered in Block 20, if different from Report)

18. SUPPLEMENTARY NOTES

19. KEY WORDS (Continue on reverse side if necessary and identify by block number)

Linearized Navier-Stokes Equations
Liquid-Filled Shell
Liquid Moment Coefficient
Liquid Pressure Moment
Liquid Payload
Liquid Spin-Up
Resonance
Rotating Fluid
Spinning Nutating Cylinder

20. ABSTRACT (Continue on reverse side if necessary and identify by block number) (bja)

A study is made of the flow of a liquid in a cylindrical container that nutates at constant frequency and small amplitude and impulsively begins spinning with a fixed angular velocity. In particular, the history of pressure overturning moment during spin-up is investigated. The partial differential equations of the problem are linearized, and a modal analysis (separated variable solution) is applied. One consequence of stipulating a modal analysis is

(continued)

DD FORM 1 JAN 73 1473 EDITION OF 1 NOV 65 IS OBSOLETE

UNCLASSIFIED

SECURITY CLASSIFICATION OF THIS PAGE (When Data Entered)

a difficulty with endwall boundary conditions; this difficulty is avoided here by specifying a heuristic boundary condition and then satisfying it approximately. Calculations indicate that peaks of overturning or restoring moment occur at or near those times when the nutational frequency is equal to one of the frequencies of inertial oscillations of the liquid. This phenomenon of resonance extends the result of Stewartson obtained for inviscid perturbations in solid body rotation.

TABLE OF CONTENTS

LIST OF ILLUSTRATIONS

I. INTRODUCTION

The study of the motion and stability of a liquid-filled projectile requires a knowledge of the internal motion of the liquid which determines the moment exerted by the liquid on the projectile. The motion of the spinning liquid can be divided into two categories: (1) solid body rotation, the condition attained for "large" time, and (2) spin-up, the transient state before solid body rotation is attained. Investigations have been directed along two lines: (1) the determination of the frequencies and decay rates of inertial oscillations, and (2) prediction of the moment on a spinning liquid-filled cylinder executing angular motion. These are referred to as the "eigenvalue problem" and "moment problem," respectively.

For solid body rotation rational theories have been developed and applied both to the eigenvalue problem[1] and to the moment problem with restrictive conditions.[2,3,4] The works of Stewartson[5] and Wedemeyer[6] form the basis of these efforts. Clearly, to include the transient spin-up effects requires a non-trivial extension of those works. Eigenfrequencies and decay rates have been obtained for spin-up;[7,8] the solutions did not satisfy the no-slip condition at the endwalls. In Reference 7 it was shown that calculated frequencies compared with experimental results to within a few percent, but decay rates could be off by as much as a factor of two. If an endwall correction for solid body rotation is applied during spin-up (obviously an ad hoc correction) the prediction of decay rate is improved for late time but not

---

1. *C. W. Kitchens, Jr., N. Gerber, and R. Sedney, "Oscillations of a Liquid in a Rotating Cylinder: Part I. Solid Body Rotation," BRL Technical Report ARBRL-TR-02081, June 1978. (AD A057759)*

2. *N. Gerber, R. Sedney, and J. M. Bartos, "Pressure Moment on a Liquid-Filled Projectile: Solid Body Rotation," BRL Technical Report ARBRL-TR-02422, October 1982. (AD A120567)*

3. *C. H. Murphy, "Angular Motion of a Spinning Projectile with a Viscous Liquid Payload," BRL Memorandum Report ARBRL-MR-03194, August 1982. (AD A118676) (See also Journal of Guidance, Control, and Dynamics, Vol. 6, July-August 1983, pp. 280-286.)*

4. *N. Gerber and R. Sedney, "Moment on a Liquid-Filled Spinning and Nutating Projectile: Solid Body Rotation," BRL Technical Report ARBRL-TR-02470, February 1983. (AD A125332)*

5. *K. Stewartson, "On the Stability of a Spinning Top Containing Liquid," Journal of Fluid Mechanics, Vol. 5, Part 4, 1959.*

6. *E. H. Wedemeyer, "Viscous Corrections to Stewartson's Stability Criterion," BRL Report No. 1287, June 1966. (AD 489687)*

7. *R. Sedney and N. Gerber, "Oscillations of a Liquid in a Rotating Cylinder: Part II. Spin-Up," BRL Technical Report ARBRL-TR-02489, May 1983. (AD A129094)*

8. *C. H. Murphy, "Moment Induced by Liquid Payload During Spin-Up Without a Critical Layer," BRL Report in preparation. Also AIAA 22nd Aerospace Sciences Meeting, Reno, Nevada, January 1984, AIAA Paper No. 84-0229.*

early time. In this paper we calculate the contribution of the pressure to the moment during spin-up of a liquid that fills a right circular cylinder undergoing coning motion at constant frequency and constant yaw angle. The contribution of the wall shear will be treated in a later report.

Two coordinate systems will be used. The first is an inertial system; i.e., the unyawed reference frame shown in Figure 1, with rectangular coordinates (x, y, z) and cylindrical coordinates (r, θ, x), where $r = (y^2 + z^2)^{1/2}$ and θ = arctan (z/y). The second reference frame will be defined later.

Here, as in previous work,[2,3,4] we assume the yaw to be sufficiently small so that a linearized analysis is applicable; i.e., the flow may be considered the sum of a basic unperturbed flow and a perturbation flow. Also we specify that the perturbed flow variables have the form*

$$e^{i[(1 - i\varepsilon)\,\tau\,\dot{\phi}\,t - \theta]}\ fn\ (r, x), \tag{1.1}$$

where t is time, τ and ε are non-dimensional nutational frequency and yaw growth rate. The τ is non-dimensionalized by $\dot{\phi}$, the spin of the cylinder; r and x are non-dimensionalized by a, the cross-sectional radius of the cylinder. This form of solution renders the problem time-independent (aside from the quasi-steady spin-up perturbation assumption, to be discussed later); and it implies that there are no transients present between the angular motion of the cylinder and the corresponding response of the flow. One would not expect this assumption to be valid early in the spin-up history of the rotating liquid, but at least it should be applicable when solid body rotation has been attained. Justification for this assumption will depend on comparison of the results with those of measurements.

The second coordinate system used to describe the projectile, Figure 1, is the $\tilde{x}$, $\tilde{y}$, $\tilde{z}$ non-spinning system which has the $\tilde{x}$ -axis along the projectile axis of symmetry; the $\tilde{y}$ and $\tilde{z}$ axes are omitted for clarity. The x = 0 and $\tilde{x}$ = 0 values are located at the midplanes of the unyawed and yawed cylinders, respectively. The $\tilde{x}$ -axis is nutating about the x-axis with the angle $K_1(t)$; the pivot point lies at the midplane. The components of the projection in the y, z plane of a unit vector lying on the $\tilde{x}$ -axis are denoted by n_{YE} and n_{ZE}, respectively. It is convenient to combine the two components of yaw into a single complex variable

$$\tilde{\xi} \equiv -(n_{YE} + i\, n_{ZE}). \tag{1.2}$$

The nomenclature here is that prescribed in Reference 3 and used in References 2 and 4.

Defintions of quantities are given in the LIST OF SYMBOLS Section.

The projectile motion is specified as:

$$\tilde{\xi} = (K_o e^{\varepsilon\tau\dot{\phi}t})\, e^{i\,(\tau\dot{\phi}t)} = K_1 e^{i\phi_1} = K_o e^{i\, f\dot{\phi}t}, \tag{1.3}$$

where

$$K_1 = K_o e^{\varepsilon\tau\dot{\phi}t}, \qquad \phi_1 = \tau\dot{\phi}t, \qquad f \equiv (1 - i\varepsilon)\,\tau\,. \tag{1.4}$$

Here K_o is the magnitude of the yaw at time $t = 0$; the yaw grows when $\varepsilon\tau > 0$. Also ϕ_1 is the angular orientation of the $\tilde{x}$-axis in the x, y, z system as shown in Figure 1.

The specified projectile motion given in Eq. (1.3) was found in gyroscope experiments to be applicable to a portion of the coning motion history in which the fluid was practically spun up.[2,4] However, this simple motion is not expected to occur very early in flight while the spin-up process is dominating the flow; thus, our model will not simulate the free-flight situation. We turn, instead, to forced coning motion and fix τ and ε as input; in particular, we choose $\varepsilon = 0$, implying no yaw growth. Emphasis will be placed on investigating resonances between the angular motion and free oscillations of the liquid.

After the t, θ portion of the solution in Eq. (1.1) is factored out, the problem is posed in the r, x plane. We attempt, as in References 2 and 4, to solve it by a modal analysis, i.e., by separation of variables. For solid-body rotation, we succeeded in obtaining a rational solution;[2] this solution required a corrected endwall boundary condition for axial velocity in order for it to satisfy the no-slip condition. Because of the simple basic flow (fluid angular velocity about the axis = $\dot{\phi}$ everywhere) the corrected boundary condition is a simple one, containing a complex constant, δc, proportional to $Re^{-1/2}$, where

$$Re \equiv a^2\dot{\phi}/\nu \tag{1.5}$$

is the Reynolds number and ν is the kinematic viscosity of the liquid.

In the present problem the basic flow is the spin-up flow, for which a corrected endwall condition is not available. The Ekman layers (see Reference 7) should be included in the basic flow but are not in the present analysis. The effect that including them would have on a separation-of-variables approach is not known at this time.

Murphy[8] has proposed a method of calculating the liquid moment which has the intent of bypassing the difficulty; namely, to apply an endwall boundary condition on the axial flow identical in form to that for solid body rotation, with the difference that the Re in the expression for the δc previously mentioned is replaced by an "effective Reynolds number," Re_E. This Reynolds number is obtained by averaging over a meridional plane some dynamic quantity of the basic spin-up flow which varies with r, e.g., azimuthal velocity or angular momentum. In this model the "corrected" endwall boundary condition for axial flow is fitted in a least squares sense.

This procedure is not a rational approximation, defined as one in which the next term in the approximation (or the error) can be calculated in principle or estimated in an order of magnitude sense. Therefore, it must be considered an ad hoc approximation. The solution satisfies an incorrect boundary condition approximately; there is no way of estimating the error in the moments. Obviously, the approximation is more valid for small departures from solid body rotation. This ad hoc procedure forms the basis of the present work.

II. FLOW PROBLEM

A. Flow Equations and Boundary Conditions.

The equations are stated and solved in the inertial frame. The flow is expressed as the sum of a basic axisymmetric spin-up flow and a perturbation:*

$$u = \overset{*}{U}(r,x,\bar{t}) - K_o \overset{*}{u}(r,\theta,x,\bar{t}) \tag{2.1a}$$

$$v = \overset{*}{V}(r,x,\bar{t}) - K_o \overset{*}{v}(r,\theta,x,\bar{t}) \tag{2.1b}$$

$$w = \overset{*}{W}(r,x,\bar{t}) - K_o \overset{*}{w}(r,\theta,x,\bar{t}) \tag{2.1c}$$

$$p = \overset{*}{P}(r,x,\bar{t}) - K_o \overset{*}{p}(r,\theta,x,\bar{t}), \tag{2.1d}$$

where $\bar{t} = \dot{\phi}t$. Here u, v, w are velocity components in the radial, azimuthal, and axial directions, respectively; $\overset{*}{U}$, $\overset{*}{V}$, $\overset{*}{W}$ are the corresponding velocity components of the basic flow which is a solution of the axisymmetric Navier-Stokes equations. The velocity components of the perturbed flow are $\overset{*}{u}$, $\overset{*}{v}$, and $\overset{*}{w}$. The quantity p is pressure, $\overset{*}{P}$ is the pressure of the basic flow, and $\overset{*}{p}$ is the perturbation pressure. Velocity is non-dimensionalized by $a\dot{\phi}$ and pressure by $\rho a^2\dot{\phi}^2$, where ρ is the density of the liquid.

The variables of Eq. (2.1) are substituted into the 3-D Navier-Stokes equations (see, e.g., Eqs. (3.33) of Reference 9) and only zeroth and first order terms in K_o are retained. At this point we make several simplifications to render the problem tractable; these steps are described in detail in Sections II and III of Reference 7. First the basic flow is approximated by

---

** The negative signs in Eq. (2) were employed to comply with the nomenclature of Reference 3.*

9. H. Schlichting, Boundary Layer Theory, McGraw-Hill Book Co., New York, NY, 1960.

the Wedemeyer model for the spin-up flow (introduced in Reference 10 and discussed further in Reference 11). In this model the flow field is divided into two regions: (1) the boundary layers adjacent to the endwalls, called the "Ekman layers," and (2) the remainder of the flow field called the "core," in which the flow variables are designated U, V, W, P. (The need for an additional boundary layer at the sidewall is discussed in Reference 11.) These satisfy the following set of equations (where subscripts denote partial differentiation):

$$V_t + U\,(V_r + V/r) = Re^{-1}\,[V_{rr} + (V/r)_r] \qquad (2.2a)$$

$$U_x = V_x = P_x = 0 \qquad \text{("Columnar" Flow)} \qquad (2.2b)$$

$$U = fn\,(r,V) \qquad (2.2c)$$

$$W = -(x/r)\,(rU)_r \qquad \text{(Continuity Equation)} \qquad (2.2d)$$

$$P_r = V^2/r \qquad (2.2e)$$

Eq. (2.2b) indicates that $V = V(r, t)$; Eq. (2.2c) is the "Ekman compatibility condition" given by Eqs. (2.8) and (2.9) of Reference 7:

$$U = \kappa\,(a/c)\,Re^{-1/2}\,(V-r) \qquad \text{for laminar Ekman layer}$$

$$U = -0.035\,(a/c)\,Re^{-1/5}\,(r-V)^{8/5} \qquad \text{for turbulent Ekman layer;}$$

$\kappa = 0.5$ will be used here. Boundary conditions for an impulsive start are

$$V\,(r = 0) = 0, \qquad V\,(r = 1) = 1, \qquad V\,(t = 0) = 0. \qquad (2.3)$$

The following linearized equations are obtained to describe viscous perturbations in the core flow but not the Ekman layers, according to the discussion preceding Eqs. (3.4) in Reference 7:

---

10. *E. H. Wedemeyer, "The Unsteady Flow Within a Spinning Cylinder," BRL Report No. 1225, October 1963. (AD 431846) (See also Journal of Fluid Mechanics, Vol. 20, Part 3, 1964, pp. 383-399.)*

11. *R. Sedney and N. Gerber, "Viscous Effects in the Wedemeyer Model of Spin-Up From Rest," BRL Technical Report ARBRL-TR-02493, June 1983. (AD A129506).*

$$\overset{*}{u}_t + (V/r)\,\overset{*}{u}_\theta - 2V\,\overset{*}{v}/r = -\overset{*}{p}_r + Re^{-1}\,(\nabla^2\overset{*}{u} - \overset{*}{u}/r^2 - 2\,\overset{*}{v}_\theta/r^2) \qquad (2.4a)$$

$$\overset{*}{v}_t + (V_r + V/r)\,\overset{*}{u} + (V/r)\,\overset{*}{v}_\theta = -\overset{*}{p}_\theta/r + Re^{-1}\,(\nabla^2\overset{*}{v} - \overset{*}{v}/r^2 + 2\overset{*}{u}_\theta/r^2) \qquad (2.4b)$$

$$\overset{*}{w}_t + (V/r)\,\overset{*}{w}_\theta = -\overset{*}{p}_x + Re^{-1}\,\nabla^2\overset{*}{w} \qquad (2.4c)$$

$$(r\overset{*}{u})_r + \overset{*}{v}_\theta + r\,\overset{*}{w}_x = 0, \qquad (2.4d)$$

where

$$\nabla^2 \equiv \partial^2/\partial r^2 + (1/r)\,\partial/\partial r + (1/r^2)\,\partial^2/\partial\theta^2 + \partial^2/\partial x^2.$$

The reasons that U and W do not appear in Eq. (2.4) are discussed in Reference 7.

The boundary conditions are: no flow through the bounding walls and no slip along them; i.e.,

$$\tilde{u}\,(\tilde{r}=1) = \tilde{w}\,(\tilde{r}=1) = 0, \qquad \tilde{v}\,(\tilde{r}=1) = 1 \qquad \text{(side)} \qquad (2.5a)$$

$$\tilde{u}\,(\tilde{x}=\pm A) = \tilde{w}\,(\tilde{x}=\pm A) = 0, \qquad \tilde{v}\,(\tilde{x}=\pm A) = \tilde{r} \qquad \text{(end)} \qquad (2.5b)$$

where $\tilde{u}$, $\tilde{v}$, $\tilde{w}$ are non-dimensional cylindrical velocity components in the $\tilde{r}$, $\tilde{\theta}$, $\tilde{x}$ system; A is the half-height, c, of the cylinder divided by a.

The boundary conditions must be transformed to the variables used in Eq. (2.4); a discussion of the transformations is given in Appendix A. The resulting non-homogeneous sidewall conditions are

$$\overset{*}{u}\,(r=1) = x\ \text{Real}\,[-i\,(1-\tau)\exp\{i\,(\dot{\tau}\phi t - \theta)\}] + O\,(K_o) \qquad (2.6a)$$

$$\overset{*}{v}\,(r=1) = -x\ \text{Real}\,[\{V_r\,(r=1) - \tau\}\exp\{i\,(\tau\dot{\phi}t - \theta)\}] + O\,(K_o) \qquad (2.6b)$$

$$\overset{*}{w}\,(r=1) = \text{Real}\,[i\,(1-\tau)\exp\{i\,(\tau\dot{\phi}t - \theta)\}] + O\,(K_o)\,. \qquad (2.6c)$$

The complex form is introduced here for later convenience.

The endwall boundary conditions for $\overset{*}{u}$, $\overset{*}{v}$, $\overset{*}{w}$ cannot be stated precisely. The U, V, and W are valid only in the core, and the Ekman layer flow which should be included in the unperturbed solution is not available. This

difficulty is responsible for the introduction of the ad hoc endwall boundary condition stated in Section I. The motion of the cylinder is expected nevertheless, to determine the t, θ dependence of boundary conditions so that

$$\overset{*}{u}\,(x = \pm A) = \text{Real}\,\{fn\,(\pm A, r)\,\exp\,[i\,(\tau\bar{t} - \theta)]\}, \tag{2.7}$$

with similar expressions for $\overset{*}{v}\,(x = \pm A)$ and $\overset{*}{w}\,(x = \pm A)$. Axial boundary conditions will be treated later.

One further approximation is needed to permit application of a modal analysis, namely, the "quasi-steady" condition discussed in Section III of Reference 7. Generally, V does not change appreciably over the time scale of the perturbations; thus $\bar{t}$ can be regarded as a parameter in the solution of Eq. (2.4). A possible exception to this might exist for $\bar{t} \to 0$ and an impulsive start.

B. Modal Analysis: Separated Variable Solutions

1. Equations and Boundary Conditions for r, x Variation. It is assumed that the perturbation can be expressed as a superposition of modes, or a triple Fourier expansion in θ, x, and t with coefficients functions of r. It is convenient to use complex notation and express the perturbation as

$$\overset{*}{u} = \text{Real}\,(\overset{*}{u}_c) = \text{Real}\,[\underline{u}\,(r, x; \bar{t})\,\exp\,\{i\,(\tau\bar{t} - \theta)\}] \tag{2.8a}$$

$$\overset{*}{v} = \text{Real}\,(\overset{*}{v}_c) = \text{Real}\,[\underline{v}\,(r, x; \bar{t})\,\exp\,\{i\,(\tau\bar{t} - \theta)\}] \tag{2.8b}$$

$$\overset{*}{w} = \text{Real}\,(\overset{*}{w}_c) = \text{Real}\,[\underline{w}\,(r, x; \bar{t})\,\exp\,\{i\,(\tau\bar{t} - \theta)\}] \tag{2.8c}$$

$$\overset{*}{p} = \text{Real}\,(\overset{*}{p}_c) = \text{Real}\,[\underline{p}\,(r, x; \bar{t})\,\exp\,\{i\,(\tau\bar{t} - \theta)\}] \tag{2.8d}$$

where $\underline{u}$, $\underline{v}$, $\underline{w}$, and $\underline{p}$ are complex functions. The functions $\overset{*}{u}_c$, $\overset{*}{v}_c$, $\overset{*}{w}_c$, and $\overset{*}{p}_c$ are clearly also solutions of Eq. (2.4). The t, θ portion of the boundary conditions in Eqs. (2.6) and (2.7) are satisfied by Eq. (2.8). Substituting $\overset{*}{u}_c$, $\overset{*}{v}_c$, $\overset{*}{w}_c$, $\overset{*}{p}_c$ from Eq. (2.8) into Eq. (2.4) yields

$$r\,\underline{u}_r + \underline{u} - i\,\underline{v} + r\,\underline{w}_x = 0 \tag{2.9a}$$

$$i\,(\tau - V/r)\underline{u} - (2V/r)\underline{v} = -\underline{p}_r + (1/\text{Re})\,[\underline{u}_{rr} + \underline{u}_r/r - 2\underline{u}/r^2 + \underline{u}_{xx} + 2i\underline{v}/r^2] \tag{2.9b}$$

$$i(\tau - V/r)\underline{v} + (V_r + V/r)\,\underline{u} = -i\underline{p}/r + (1/Re)\,[\underline{v}_{rr} + \underline{v}_r/r - 2\underline{v}/r^2 + \underline{v}_{xx} - 2i\underline{u}/r^2] \tag{2.9c}$$

$$i(\tau - V/r)\underline{w} = -\underline{p}_x + (1/Re)\,[\underline{w}_{rr} + w_r/r - \underline{w}/r^2 + \underline{w}_{xx}]. \tag{2.9d}$$

Boundary conditions at the axis are

$$\underline{u}\,(r = 0) - i\underline{v}\,(r = 0) = w\,(r = 0) = \underline{p}\,(r = 0) = 0. \tag{2.10}$$

These are kinematic conditions, stated in Eq. (4.3) of Reference 7, for m = 1. Boundary conditions at the sidewall are

$$\underline{u}\,(r = 1) = -i(1 - \tau)x \tag{2.11a}$$

$$\underline{v}\,(r = 1) = -\{V_r(r = 1) - \tau\}x \tag{2.11b}$$

$$\underline{w}\,(r = 1) = i(1 - \tau). \tag{2.11c}$$

At this point we invoke the ad hoc endwall boundary condition, namely

$$\underline{w} \mp \delta c_E\, \partial\underline{w}/\partial x = i\,(1 - \tau)\,r \qquad \text{at} \qquad x = \pm A, \tag{2.12}$$

with the left-hand side identical in form to that of Eq. (29) of Reference 2; namely, the corrected homogeneous endwall boundary condition. The right-hand side is the same as that of the uncorrected inhomogeneous boundary condition of Eq. (A.10). The δc_E is found as follows:

$$\alpha_E = 2^{-1/2}\, Re_E^{1/2}\,(1 - i)\,(3 - \tau)^{1/2} \tag{2.13a}$$

$$\beta_E = 2^{-1/2}\, Re_E^{1/2}\,(1 + i)\,(1 + \tau)^{1/2} \tag{2.13b}$$

$$\delta c_E = \left[\frac{1}{2\alpha_E}\left(1 - \frac{2}{1 - \tau}\right) + \frac{1}{2\beta_E}\left(1 + \frac{2}{1 - \tau}\right)\right], \tag{2.13c}$$

with the restriction $(3 - \tau) \geq 0$. The "effective" Reynolds number used here is given by

$$Re_E(\bar{t}) = \left[2 \int_0^1 V\,(r;\bar{t})\, dr \right] a^2 \dot{\phi}/\nu. \tag{2.14}$$

For solid body rotation, with $V = r$, the bracketed term is equal to unity and $Re_E = Re$. While the fluid is spinning up, $V < r$, and $Re_E < Re$. As an example, $Re_E/Re = 0.76$ at $\bar{t} = 1000$ for the case $Re = 39772$, $c/a = 3.12$.

2. Form of Solution. As in Section III-B of Reference 2, we stipulate that the solution be a linear combination of separated variable solutions, i.e.,

$$\left.\begin{aligned} \underline{u} &= \Sigma\, R_u(r)\, X_u(x) & \underline{w} &= \Sigma\, R_w(r)\, X_w(x) \\ \underline{v} &= \Sigma\, R_v(r)\, X_v(x) & \underline{p} &= \Sigma\, R_p(r)\, X_p(x). \end{aligned}\right\} \tag{2.15}$$

Substituting these into Eq. (2.9) yields ordinary differential equations for the R's and X's. The X's must satisfy the harmonic equation

$$d^2X/dx^2 + \lambda^2 X = 0, \tag{2.16}$$

where λ can be zero or finite. When λ is finite, it is determined from an axial eigenvalue problem and labeled with the index k.

In this work we choose to express the solution as

$$\underline{u} = \hat{u}_o(r)\, x + \sum_{k=1}^{KF} \hat{u}_k(r) \sin \lambda_k x + \sum_{j=1}^{NJ} d_j\, \bar{u}_j(r) \sin \mu_j x \tag{2.17a}$$

$$\underline{v} = \hat{v}_o(r)\, x + \sum_{k=1} \hat{v}_k(r) \sin \lambda_k x + \sum_{j=1} d_j\, \bar{v}_j(r) \sin \mu_j x \tag{2.17b}$$

$$\underline{w} = \hat{w}_o(r) - \sum_{k=1} \hat{w}_k(r) \cos \lambda_k x - \sum_{j=1} d_j\, \bar{w}_j(r) \cos u_j x \tag{2.17c}$$

$$\underline{p} = \hat{p}_o(r)\, x + \sum_{k=1} \hat{p}_k(r) \sin \lambda_k x + \sum_{j=1} d_j\, \bar{p}_j(r) \sin \mu_j x, \tag{2.17d}$$

where the λ_k's form a denumerable set of solutions to the functional equation (See Eq. (31) of Reference 2)

$$\cos \lambda_k A + \lambda_k \delta c_E \sin \lambda_k A = 0. \tag{2.18}$$

For $|\delta c_E|/A \ll 1$,

$$\lambda_k \simeq (k\pi)/[2\ (A - \delta c_E)]. \qquad \underline{k \text{ odd}} \tag{2.19}$$

Thus, at the endwall each $\hat{w}_k(r) \cos \lambda_k x$ term in Eq. (2.17c) satisfies Eq. (2.12) with the right-hand side replaced by zero.

The μ_j's are eigenvalues of the radial differential equations resulting from separation of variables, with homogeneous sidewall boundary conditions:

$$\bar{u}_j\ (r = 1) = \bar{v}_j\ (r = 1) = \bar{w}_j(r = 1) = 0. \tag{2.20}$$

The parameter τ enters here in the same way as the unknown eigenvalue C in Reference 7. In the present situation τ is known and μ_j is the eigenvalue to be determined. The d_j's are constants to be determined so as to minimize the error in satisfying the endwall boundary condition, Eq. (2.12). The homogeneous boundary conditions, Eqs. (2.10) and (2.20), do not produce unique eigenfunctions $\bar{u}_j$, $\bar{v}_j$, $\bar{w}_j$, and $\bar{p}_j$; these are known to within a common constant. The functional values obtained from the integration are a result of the values assigned the non-homogeneous quantities at r = 0. The subsequent determination of the d_j's, however, renders the flow solution unique.

The $\hat{u}_o$, $\hat{v}_o$, $\hat{w}_o$, $\hat{p}_o$, corresponding to $\lambda = 0$, satisfy the sidewall conditions (the same as for the particular solution in Reference 2)

$$\hat{u}_o\ (r = 1) = -i\ (1-\tau)^2/(1+\tau) \tag{2.21a}$$

$$\hat{v}_o\ (r = 1) = -[(1-\tau)^2/(1+\tau)] \tag{2.21b}$$

$$\hat{w}_o\ (r = 1) = i\ (1-\tau). \tag{2.21c}$$

This set of conditions was chosen so that $\hat{w}_o$ satisfied the total boundary condition at r = 1, Eq. (2.11c); better conditions on $\hat{u}_o(1)$ and $\hat{v}_o(1)$ might be selected, and alternate choices are being considered. The sidewall boundary

conditions for second terms of the solution, Eq. (2.17), are obtained by subtracting the expressions of Eq. (2.21) (times x for $\hat{u}_o$ and $\hat{v}_o$) from those of Eq. (2.11):

$$\Sigma\, \hat{u}_k\ (r = 1) \sin \lambda_k x = -i\ [2\tau\ (1-\tau)/(1+\tau)]\ x \tag{2.22a}$$

$$\Sigma\, \hat{v}_k\ (r = 1) \sin \lambda_k x = [\{(1-\tau)^2/(1+\tau)\} - V_r\ (r = 1) + \tau]\ x \tag{2.22b}$$

$$\Sigma\, \hat{w}_k\ (r = 1) \cos \lambda_k x = 0. \tag{2.22c}$$

For solid body rotation the d_j's vanish and the remainder of the solution, Eq. (2.17), is the same as that in Reference 2.

3. Radial Variation Problem. When each individual term of Eq. (2.17) is substituted into Eq. (2.9), a system of linear ordinary equations in r of the following form, omitting subscripts k on the dependent variables, is obtained, (where ' $\equiv$ d/dr):

$$r\,\hat{u}' + \hat{u} - i\hat{v} + \lambda_k\, r\hat{w} = 0 \tag{2.23a}$$

$$\mathrm{Re}^{-1}\,\hat{u}'' + (\mathrm{Re}\ r)^{-1}\,\hat{u}' + [i\ (V/r - \tau) - \mathrm{Re}^{-1}\ (2/r^2 + \lambda_k{}^2)]\,\hat{u} + [2\ V/r + 2i\ (\mathrm{Re}\ r^2)^{-1}]\,\hat{v} = \hat{p}' \tag{2.23b}$$

$$\mathrm{Re}^{-1}\,\hat{v}'' + (\mathrm{Re}\ r)^{-1}\,\hat{v}' + [i\ (V/r - \tau) - \mathrm{Re}^{-1}\ (2/r^2 + \lambda_k{}^2)]\,\hat{v} - [V/r + V_r + 2i\ (\mathrm{Re}\ r^2)^{-1}]\,\hat{u} = -i\,\hat{p}/r \tag{2.23c}$$

$$\mathrm{Re}^{-1}\,\hat{w}'' + (\mathrm{Re}\ r)^{-1}\,w' + [i\ (V/r - \tau) - \mathrm{Re}^{-1}\ (1/r^2 + \lambda_k{}^2)]\,\hat{w} = -\lambda_k\,\hat{p} + \varepsilon_p\,\hat{p}. \tag{2.23d}$$

The quantity ε_p is equal to 1 when $\lambda_k = 0$; otherwise, it is zero. The same equations apply to $\bar{u}_j$, $\bar{v}_j$, $\bar{w}_j$, $\bar{p}_j$, with λ_k replaced by μ_j.

These equations are converted to canonical form in order to be integrated numerically; i.e.,

$$y_i' \equiv dy_i/dr = f_i\ (r, y_1, y_2, \ldots y_6), \quad i = 1,2,\ldots,6,$$

where

$$\left.\begin{aligned} y_1 &= \hat{u}\ (\text{or } \bar{u}) & y_4 &= \hat{w}\ (\text{or } \bar{w}) \\ y_2 &= \hat{u} - i\hat{v}\ (\text{or } \bar{u} - i\bar{v}) & y_5 &= \hat{w}'\ (\text{or } \bar{w}') \\ y_3 &= \hat{v}'\ (\text{or } \bar{v}') & y_6 &= \hat{p}\ (\text{or } \bar{p}). \end{aligned}\right\} \tag{2.24}$$

After the required manipulations are performed, the following sixth order system is obtained for the $\hat{u}$, $\hat{v}$, $\hat{w}$, $\hat{p}$ case:

$$y_1' = (y_2/r) - \lambda_k\, y_4 \tag{2.25a}$$

$$y_2' = -(y_2/r) - i\, y_3 - \lambda_k\, y_4 \tag{2.25b}$$

$$y_3' = [\mathrm{Re}\,(V/r + V_r) + 2i/r^2]\, y_1 + i\,(B + 1/r^2)\,(y_2 - y_1) - y_3/r - i\,(\mathrm{Re}/r)\, y_6 \tag{2.25c}$$

$$y_4' = y_5 \tag{2.25d}$$

$$y_5' = B\, y_4 - y_5/r - \lambda_k\, \mathrm{Re}\, y_6 + \varepsilon_p\, \mathrm{Re}\, y_6 \tag{2.25e}$$

$$y_6' = -B\, y_1/\mathrm{Re} + (i/\mathrm{Re})\,[2\,\mathrm{Re}\, V/r + i/r^2]\,(y_2 - y_1) + i\, y_3/(r\,\mathrm{Re}) - \lambda_k\, y_5/\mathrm{Re}, \tag{2.25f}$$

where

$$B \equiv (1/r^2) + \lambda_k^2 + i\,\mathrm{Re}\,[\tau - V/r]. \tag{2.26}$$

The λ_k's are replaced by μ_j's for the $\bar{u}$, $\bar{v}$, $\bar{w}$, $\bar{p}$ case.

4. Boundary Conditions for Radial Equations. There are three boundary conditions at r = 0 and three at r = 1. As a consequence of Eqs. (2.10), (2.17), and (2.24), conditions at r = 0 are

$$\left.\begin{aligned} y_{2k}(0) = y_{4k}(0) = y_{6k}(0) = 0 \\ y_{2j}(0) = y_{4j}(0) = y_{6j}(0) = 0. \end{aligned}\right\} \tag{2.27}$$

In Eq. (2.22) the function x can be expanded in the series

$$x = \sum_k b_k \sin \lambda_k x, \tag{2.28}$$

where the coefficients, given by Eq. (40) in Reference 2, are

$$b_k = \frac{(2/\lambda_k^2)\,[1 + (\lambda_k\,\delta c_E)^2]\sin \lambda_k A}{A\,[1 + (\lambda_k\,\delta c_E)^2] - \delta c_E}. \tag{2.29}$$

These are the coefficients in a series of biorthogonal functions determined by solving a non-self-adjoint system, Eq. (2.16). By applying Eqs. (2.21), (2.22), (2.24), and (2.29), we obtain the following sidewall conditions for the $\hat{u}_k$, $\hat{v}_k$, $\hat{w}_k$, $\hat{p}_k$ case:

$$y_{1k}(1) = -i\,(1-\varepsilon_p)\,[2\tau\,(1-\tau)/(1+\tau)]\,b_k - i\,\varepsilon_p\,[(1-\tau)^2/(1+\tau)] \tag{2.30a}$$

$$y_{2k}(1) = -i\,(1-\varepsilon_p)\,[1 - V_r(1)]\,b_k \tag{2.30b}$$

$$y_{4k}(1) = i\,\varepsilon_p\,(1-\tau). \tag{2.30c}$$

For the eigenvalue problem solutions, $\bar{u}_j$, $\bar{v}_j$, $\bar{w}_j$, $\bar{p}_j$ case,

$$y_{1j}(1) = y_{2j}(1) = y_{4j}(1) = 0. \tag{2.30d}$$

5. Endwall Boundary Condition. When we substitute the $\underline{w}$ solution, Eq. (2.17c) evaluated at $x = \pm A$, into Eq. (2.12) and apply Eq. (2.18) to the $\hat{w}_k \cos \lambda_k x$ terms, we arrive at the following endwall boundary condition:

$$F(r, \pm A) \equiv \psi(r) - \sum_{j=1}^{NJ} d_j \bar{w}_j(r) (\cos \mu_j A + \delta c_E \mu_j \sin \mu_j A) = 0, \tag{2.31}$$

where

$$\psi(r) = \hat{w}_o(r) - i (1-\tau) r = \psi_R + i \psi_I \tag{2.32}$$

and

$$F = F_R + i F_I. \tag{2.33}$$

As discussed in Section I, Eq. (2.31) is not satisfied exactly; instead we determine a set of d_j's which will minimize

$$g(d_1, d_2, \ldots d_{NJ}) \equiv \int_0^1 (F_R^2 + F_I^2)\, dr. \tag{2.34}$$

A derivation of the formulas for the d_j's is given in Appendix B. Thus, the ad hoc endwall boundary condition is satisfied approximately, to within the accuracy of a least squares fit. An estimate of the relative error is given by the quantity

$$Er = [g / \int_0^1 (\psi_R^2 + \psi_I^2)\, dr]^{1/2}. \tag{2.35}$$

Error estimates have been computed, but we defer the presentation of results to a later report.

C. Operational Procedures.

The procedure for solving the radial ordinary differential equations, Eq. (2.25), is discussed in detail in Reference 1 for solid-body rotation and in Reference 7 for spin-up. Numerical integration must begin at a small finite value, $r = \varepsilon_o$, where three independent power-series solutions are evaluated. Due to the stiffness of the equations at large Re, the Runge-Kutta integration must be combined with orthonormalization of the three solutions in order to maintain their linear independence and prevent runaway amplitude growth. Both homogeneous and inhomogeneous sidewall conditions are encountered in this study. Reference 1 provides details of the application of the homogeneous conditions, and Reference 2 describes the treatment of the non-homogeneous conditions. The iterative procedure for computing eigenvalues is described in Section V of Reference 7.

Because the calculation of the μ_j eigenvalues forms part of our operations, it is most feasible to begin the determination of a spin-up moment history at a very large time, near solid body rotation, where initial guesses for the eigenvalues are readily available. These are found in tables (see, e.g., p. 31 of Reference 3). The operation procedes step-by-step from larger to smaller values of time, with initial guesses for the eigenvalues at each time step obtained from those at previous times.

For large t the μ_j's can be ordered (j = 1,2, etc) either by the real parts of the μ_j's or the number of zeros in their corresponding eigenfunctions. The mode is then identified by the value of j. However, as t becomes small, some of the Real (μ_j) vs t curves often intersect, rendering the ordering by Real (μ_j) inapplicable. At these times identification of the modes can become ambiguous. What frequently happens is that the iterative process converges to the solution of a mode other than the one sought because the initial estimate was not close enough to the desired eigenvalue. Operationally, this can lead to a particular mode appearing more than once in the expansion $\Sigma\, d_j\, u_j\,(r) \sin \mu_j\, x$, etc (Eq. 2.17a)). We can remove one of the duplicate terms from the series, but we are then left with fewer functions for approximating the endwall boundary condition. As the calculation proceeds for decreasing time, the number of eigenfunctions decreases by one. The error, Er, then increases.

Another possible source of difficulty at early time occurs when $M \equiv \tau - V/r = 0$, i.e., when the nutational frequency equals the frequency of the circumferential motion of the fluid, indicating a resonance; see References 7 and 12. The value of r for which M vanishes is called the "critical level" and is denoted by r_c; the neighboring region is called the "critical layer." The critical level begins at r = 1 for t = 0 and moves inward with increasing time until it reaches the axis at a finite time and then disappears. When inviscid perturbations are treated for constant yaw, as in Reference 8, the flow equations become singular at $r = r_c$. The critical layer is discussed in References 7 and 12 for viscous perturbations. Figure 4c in Reference 7 illustrates in this situation that high-frequency large amplitude oscillations in the flow solution occur about $r = r_c$ under certain conditions; the numerical process described in Reference 7 is able to compute these oscillations. The number of zeros becomes large and identification of a mode is again made ambiguous.

III. LIQUID PRESSURE MOMENT

A. Pressure and Moment Formulas.

According to Eqs. (2.1d) and (2.8d) the pressure is

---

12. *R. Sedney and N. Gerber, "Numerical Study of the Critical Layer in a Rotating Fluid," AIAA 22nd Aerospace Sciences Meeting, Reno, Nevada, January 1984, AIAA Paper No. 84-0342.*

$$p = P - K_o \left[-p_I \sin(\tau\dot{\phi}t-\theta) + p_R \cos(\tau\dot{\phi}t-\theta)\right] + O(K_o^2), \tag{3.1}$$

where

$$p(r,x) = p_R + i\, p_I. \tag{3.2}$$

Omitting the despin torque, one can express the moment produced by the liquid on the spinning and nutating shell as the complex quantity $M_{(L\tilde{Y})P} + i\, M_{(L\tilde{Z})P}$.

A complex moment coefficient, $C_{(LM)P}$, is introduced as in Eqs. (5) and (6) of Reference 2:

$$M_{(L\tilde{Y})P} + i\, M_{(L\tilde{Z})P} = (2\pi\rho a^2 c)\, a^2\dot{\phi}^2\, \tau\, C_{(LM)P}\, K_1\, e^{i\tau\dot{\phi}t} \tag{3.3}$$

$$C_{(LM)P} = C_{(LSM)P} + i\, C_{(LIM)P}.$$

The $C_{(LSM)P}$ and $C_{(LIM)P}$ represent the moments acting to change the yaw angle and the nutation rate, respectively.

The moment will be evaluated about the center of gravity of the projectile in the $\tilde{x}$, $\tilde{y}$, $\tilde{z}$ system. Details need be shown for only one component, say $M_{(L\tilde{Z})P}$, because of axisymmetry in the transverse motion. Let

$$M_{(L\tilde{Z})P} = M_{(L\tilde{Z}S)P} + M_{(L\tilde{Z}T)P} + M_{(L\tilde{Z}B)P}. \tag{3.4}$$

where the three terms on the right-hand side denote the moments on the side, top, and bottom walls, respectively; as given in Eq. (53) of Reference 2 they are

$$M_{(L\tilde{Z}S)P} = (\rho a^5\dot{\phi}^2)\left[\int_{-A}^{A}\int_{0}^{2\pi} p(\tilde{r}=1)\,\tilde{x}\cos\tilde{\theta}\, d\tilde{\theta}\, d\tilde{x}\right] \tag{3.5a}$$

$$M_{(L\tilde{Z}T)P} = -(\rho a^5\dot{\phi}^2)\left[\int_{0}^{1}\int_{0}^{2\pi} p(\tilde{x}=A)\,\tilde{r}^2\cos\tilde{\theta}\, d\tilde{\theta}\, d\tilde{r}\right] \tag{3.5b}$$

$$M_{(L\tilde{Z}B)P} = (\rho a^5\dot{\phi}^2)\left[\int_{0}^{1}\int_{0}^{2\pi} p(\tilde{x}=-A)\,\tilde{r}^2\cos\tilde{\theta}\, d\tilde{\theta}\, d\tilde{r}\right]. \tag{3.5c}$$

The non-dimensional cylinder radius occurring in the integrand of Eq. (3.5a) is equal to 1.

B. Sidewall Moment.

The pressure must be evaluated at $\tilde{r} = 1$. The bracketed term in Eq. (3.1) may be evaluated at $r = 1$ without changing the order of the approximation. According to Eq. (A4)

$$P(\tilde{r} = 1) = P(r = 1) - K_o x \cos(\tau\dot{\phi}t - \theta)(\partial P/\partial r)_{r=1}.$$

$P(r = 1)$ is a constant, designated by P_1. From Eq. (2.2e), $(\partial P/\partial r)_{r=1} = (V^2/r)_{r=1} = 1$. Hence

$$P(\tilde{r} = 1) = P(r = 1) - K_o x \cos(\tau\dot{\phi}t - \theta). \tag{3.6}$$

Then, from Eqs. (2.1d), (2.8d), and (3.6), with P replacing $\overset{*}{P}$,

$$p(\tilde{r} = 1) = P_1 - K_o \{[x + \underline{p}_R(1,x)] \cos(\tau\dot{\phi}t - \theta) - \underline{p}_I(1,x) \sin(\tau\dot{\phi}t - \theta)\} + O(K_o^2). \tag{3.7}$$

When Eq. (3.7) is substituted into Eq. (3.5a), the P_1 term makes no contribution to the integral, leaving only K_o terms; thus $\tilde{r}$, $\tilde{\theta}$, $\tilde{x}$ can be replaced by r, θ, x without changing the order of approximation. Then Eq. (3.5a) reduces to

$$M_{(L\tilde{Z}S)P}/(K_o \rho a^5 \dot{\phi}^2) = -[2\pi \text{ Real } (I_S)] \sin \tau\dot{\phi}t - [2\pi \text{ Imag } (I_S)] \cos \tau\dot{\phi}t \tag{3.8}$$

where

$$I_S = i A^3/3 + i \int_0^A x \underline{p}(1,x)\, dx. \tag{3.9}$$

Upon substitution of Eq. (2.17d), Eq. (3.9) becomes

$$I_S = \frac{i}{3} A^3 [\hat{p}_o(1) + 1] + i \sum_{k=1} \hat{p}_k(1)[\frac{1}{\lambda_k^2} \sin \lambda_k A - \frac{1}{\lambda_k} A \cos \lambda_k A] + \tag{3.10}$$

$$i \sum_{j=1}^{NJ} d_j \bar{p}_j(1) [\frac{1}{\mu_j^2} \sin \mu_j A - \frac{1}{\mu_j} A \cos \mu_j A].$$

C. Endwall Moments.

The term P(r) of Eq. (3.1) must be evaluated as a function of $\tilde{r}$, $\tilde{\theta}$ at $\tilde{x}$ = A in the moment integral of Eq. (3.5b) for the top endwall. As demonstrated in Appendix A, Eq. (A7),

$$P(r) = P(\tilde{r}) - K_o A (V^2/r) \cos (\tau\dot{\phi}t - \theta) + O(K_o^2). \tag{3.11}$$

The $P(\tilde{r})$ term makes no contribution to the integral, leaving only terms of $O(K_o)$; then the $\tilde{r}$, $\tilde{\theta}$, $\tilde{x}$ may be replaced by r, θ, x without changing the order of approximation. The remaining part of the pressure is an odd function of x; thus, the total endwall moment, $M_{(L\tilde{Z}E)P} \equiv M_{(L\tilde{Z}T)P} + M_{(L\tilde{Z}B)P} = 2\, M_{(L\tilde{Z}T)P}$.

Eqs. (3.1) and (3.11) are substituted into Eq. (3.5b) to yield

$$M_{(L\tilde{Z}E)P}/(\rho a^5 \dot{\phi}^2) = 2\pi K_o \{[\text{Imag } (I_E)] \cos \tau\dot{\phi}t + [\text{Real } (I_E)] \sin \tau\dot{\phi}t\} \tag{3.12}$$

where

$$I_E = i \int_0^1 r^2 [p\ (r, x = A) + A\, V^2/r]\, dr. \tag{3.13}$$

Substituting Eq. (2.17d) into Eq. (3.13) gives

$$I_E = \int_0^1 r^2 [A \hat{p}_o\ (r) + \sum_{k=1} \hat{p}_k\ (r) \sin \lambda_k A + \tag{3.14}$$

$$\sum_{j=1}^{NJ} d_j \bar{p}_j\ (r) \sin \mu_j A + i A V^2/r]\, dr.$$

D. Moment Coefficients.

The moments of Eqs. (3.8) and (3.12) have the form

$$M_{(L\tilde{Z}S)P} = -K_o\,(M_{1S} \sin \tau\dot{\phi}t + M_{2S} \cos \tau\dot{\phi}t)\,(\rho a^5\dot{\phi}^2)$$

$$M_{(L\tilde{Z}E)P} = -K_o\,(M_{1E} \sin \tau\dot{\phi}t + M_{2E} \cos \tau\dot{\phi}t)\,(\rho a^5\dot{\phi}^2), \tag{3.15}$$

where

$$M_{1S} = 2\pi \text{ Real } (I_S), \qquad M_{2S} = 2\pi \text{ Imag } (I_S)$$

$$M_{1E} = -2\pi \text{ Real } (I_E), \qquad M_{2E} = -2\pi \text{ Imag } (I_E).$$

The total moment is

$$M_{(L\tilde{Z})P} = M_{(L\tilde{Z}S)P} + M_{(L\tilde{Z}E)P} = -K_o\,(\rho a^5\dot{\phi}^2)\,(M_1 \sin \tau\dot{\phi}t + M_2 \cos \tau\dot{\phi}t), \tag{3.16}$$

where

$$M_1 = M_{1S} + M_{1E}, \qquad M_2 = M_{2S} + M_{2E}. \tag{3.17}$$

Our computational results will be exhibited in terms of the moment coefficient, $C_{(LM)P}$, defined in Eq. (3.3). By Eqs. (3.3), (3.16), and (3.17),

$$C_{(LSM)P} = -M_1/[2\pi\tau\ c/a], \qquad C_{(LIM)P} = -M_2/[2\pi\tau\ c/a]. \tag{3.18}$$

Our primary interest lies in $C_{(LSM)P}$, which represents overturning moment, and we shall present time histories of this quantity.

IV. RESULTS

This report does not include the contribution to the moment from the shear forces which, as shown in References 3 and 4, can be significant at lower Re; shear contribution will be treated in a subsequent work. For the present we concentrate on the analysis of the flow problem and procedures for solving it, which are needed for both pressure and shear contributions. The results given here illustrate the procedure and are compared with those of inviscid perturbation calculations by the method of Murphy.[8] Side pressure moment coefficient histories are presented for four combinations of Re and c/a.

In Case A, Figure 2, $C_{(LSM)P}$ histories are shown for five nutational frequencies: τ = 0.04, 0.05, 0.09, 0.12, and 0.14. The curves have very pronounced peaks for τ = 0.05, 0.09, 0.12, and 0.14. These peaks (except for the right-hand peaks on the τ = 0.12 and τ = 0.14 curves) occur at times close to those at which the perturbing motion is in resonance with the wave motion of the n = 1, k = 3 natural oscillation mode of the liquid in the cylinder.* The right-hand peaks on the τ = 0.12 and τ = 0.14 curves indicate resonance with the n = 2, k = 5 mode of the spinning fluid. The eigenfrequency of the n = 1, k = 3 mode is approximately C_R = 0.04 for solid body rotation; consequently the moment will not damp out with increasing time for τ = 0.04. Outputs of the inviscid perturbation calculations (method of Reference 8) are also presented for τ = 0.04, 0.05, and 0.09. The predictions of times of peak moments differ by less than 0.07 s. between the two methods. For τ = .12 and .14 only the present results are shown. Reference 8 cannot compute these cases because of the presence of the critical layer.

The results for Case B are shown in Figure 3. The spin-up time (defined in Section I of Reference 11) is smaller here than in Case A; therefore, the interval of interest occurs for smaller $\bar{t}$. The results are qualitatively the same, however. The maximum of $C_{(LSM)P}$ occurs near the time when $C_R = \tau = 0.15$ for the k = 3, n = 1 mode. The results from the method of Reference 8 are also shown in Figure 3. These disagree with the present results at $\bar{t} \cong 200$. For smaller $\bar{t}$ that method breaks down because of the existence of the critical layer. Our calculation was not carried out for smaller times because of difficulties, described in Section II.C, which were encountered in evaluating the μ_j's.

In Case C the high Reynolds number requires a turbulent Ekman layer. The aspect-ratio and nutational frequency are chosen so that $C_R(t) = \tau$ at $\bar{t} \cong$ 38,500 for the k = 5, n = 1 mode. Both methods exhibit the occurrence of resonance near this time. The critical layer occurs beyond the range of these curves in this graph.

The only difference between the parameters of Case C and Case D, Figure 5, is a 2.55% increase in aspect ratio, yet the moment coefficient histories are radically different. Sensitivity to aspect ratio has been noted previously in yaw growth rates of projectiles containing liquid payloads in solid-body rotation; see, e.g., Figures 10 and 12 in Reference 4. Both methods show yaw damping moments at this stage of the spin-up, with maximum damping near the time when $C_R = \tau$; however, the amplitudes differ widely. Furthermore, the curve of Murphy's method exhibits a period of sharply rising and falling overturning moment which the present method does not. The results of Case D are not yet thoroughly understood. The following comments may be relevant to

---

The reader is referred to References 1 and 7 for description of the oscillation modes of a liquid cylinder. In this study spin-up eigenvalues were computed without endwall boundary condition correction.

the situation. Because the cylinder is executing forced rather than free angular motion, the liquid may under certain conditions exert a yaw damping moment. The current treatment of the endwall boundary condition would lead one to infer that the theory grows less valid with decreasing time. In the inviscid perturbation method the results may deteriorate, when operating backwards in time, before the critical layer first appears.

For each perturbing frequency there is a time $t = t_M$ at which the moment coefficient has a maximum, $C_{(LSM)PM}$. Conversely, at each time there is a perturbing frequency τ_M (t) for which $C_{(LSM)P} = C_{(LSM)PM}$. For Case A Figure 6 exhibits the upper limit to the side moment coefficient that can be experienced during spin-up compared to that which can be experienced for fully spun-up basic flow. The moment coefficient ratio decreases rapidly with decreasing time in the present calculation, but the inviscid perturbation result indicates a very slowly changing ratio.

V. SUMMARY

The interaction between the flow of a liquid payload and the motion of the spinning and nutating shell containing it complicates the prediction of the angular motion of the projectile and the forces on it. This paper represents a first effort using linearized fully viscous equations to determine side pressure moments exerted by the liquid on the container during the liquid spin-up process. The heuristic approach of Murphy[8] is used which makes crucial assumptions regarding time-dependence of the flow and the endwall boundary condition. The statement of the problem specifies the angular motion of the projectile; thus, the present treatment cannot simulate actual flight, although it can simulate performable gyroscope experiments.

Calculations were made for four cases. It is seen that yaw damping moments exist under certain circumstances. For three cases good qualitative agreement is obtained with the results of inviscid perturbation calculations. Side-moment coefficient histories are bell-shaped curves with peaks occurring approximately at times when the nutational frequency coincides with an eigenfrequency of the liquid. (For the solid-body rotation resonance case in Figure 2 the curve has a flat top.) In the fourth case the discrepancy between the results of the two methods is large, though both methods predict sharp peaks of damping moment coefficient.

The next step in this investigation is to compute shear force on the cylinder walls and then obtain the shear moment on the projectile. It is expected to have a noticeable effect for smaller Reynolds numbers. Inclusion of the Ekman layers in the basic flow is necessary in order to have a rational approximation to the solution.

ACKNOWLEDGMENTS

The author wishes to thank Ms. Joan M. Bartos for her work on a large number of tasks that made the program used here operational. Her programming and editing were essential to the completion of this work. Appreciation is extended to Dr. Raymond Sedney for his general overall guidance. The moment data for inviscid perturbation were obtained from calculations performed with a program prepared by Mr. James Bradley.

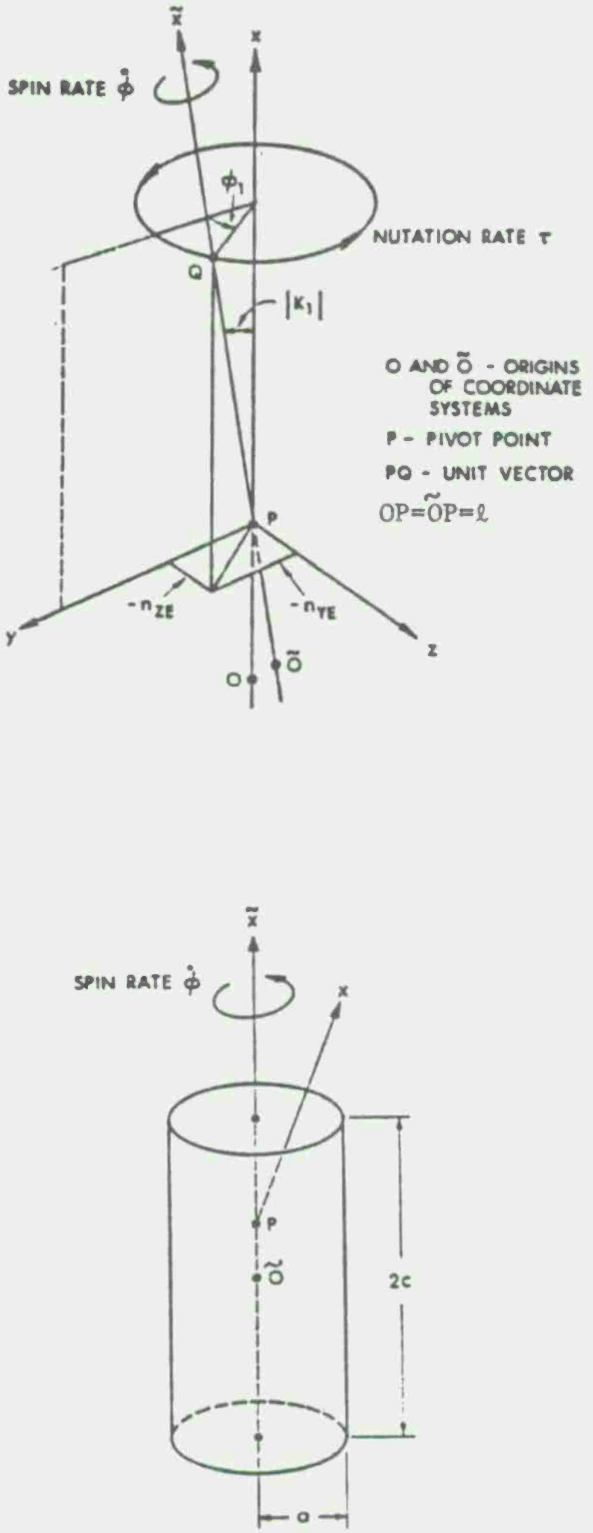

Figure 1. Diagrams of Coordinates and Cylinder.

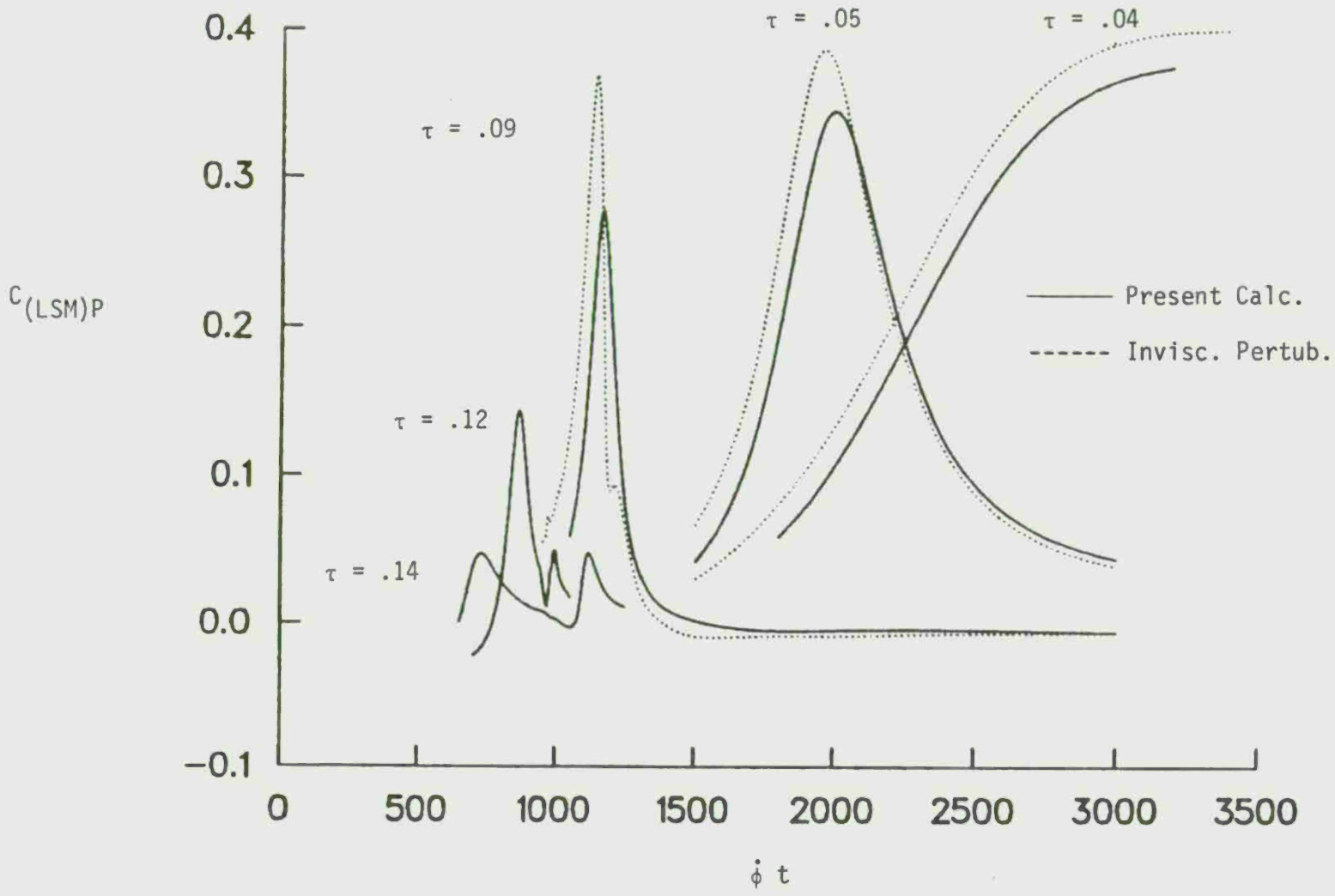

Figure 2. Side Moment Coefficient Histories for Five Nutational Frequencies, Case A: Re = 39772, c/a = 3.12, $\dot{\phi}$ = 754 rad/s.

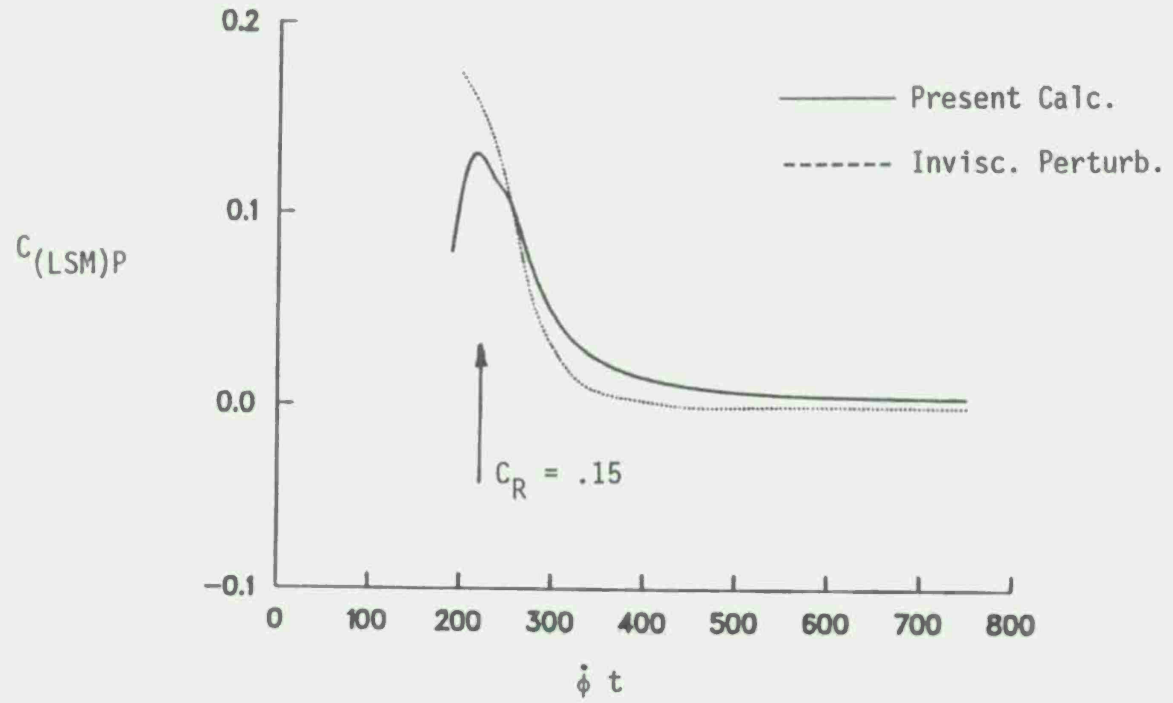

Figure 3. Side Moment Coefficient History, Case B: Re = 4974, c/a = 3.30, $\dot{\phi}$ = 8937 rad/s, τ = 0.15.

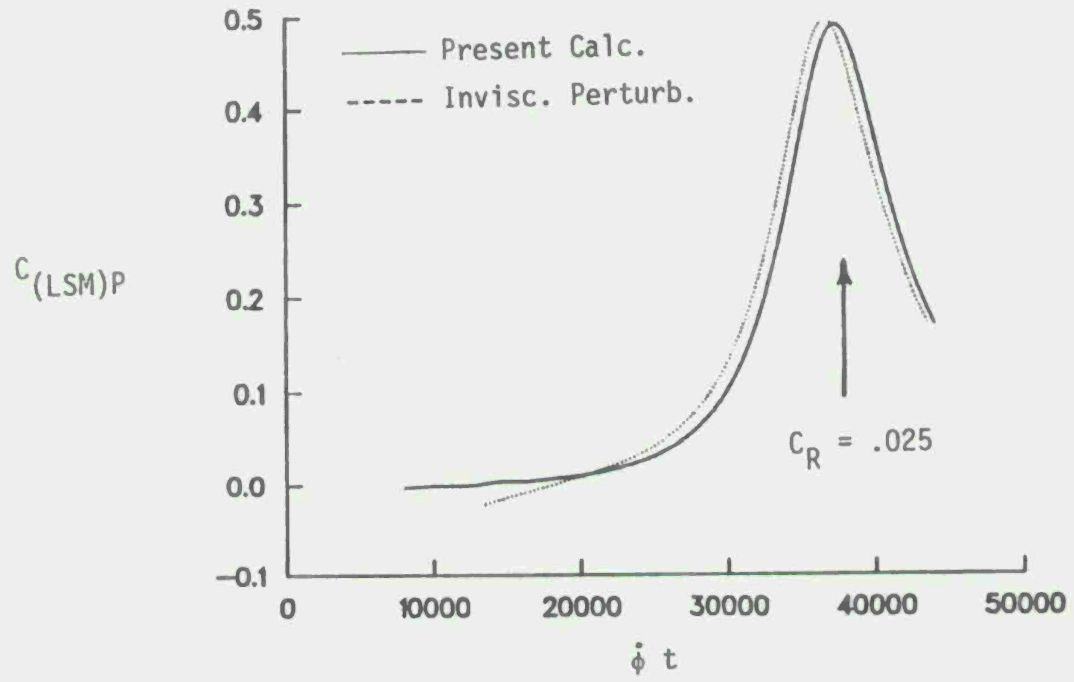

Figure 4. Side Moment Coefficient History, Case C: Re = 1.85 x 10^6, c/a = 5.100, $\dot{\phi}$ = 641 rad/s, τ = 0.025.

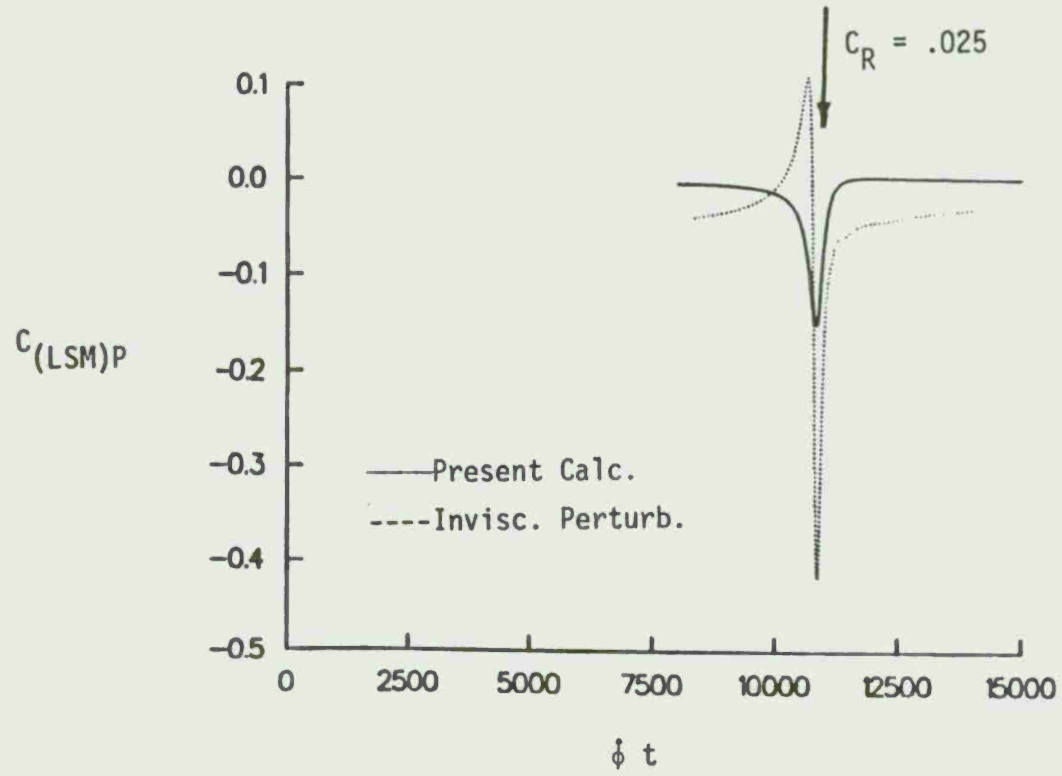

Figure 5. Side Moment Coefficient History, Case D: Re = 1.85 x 10^6, c/a = 4.973, $\dot{\phi}$ = 641 rad/s, τ = 0.025.

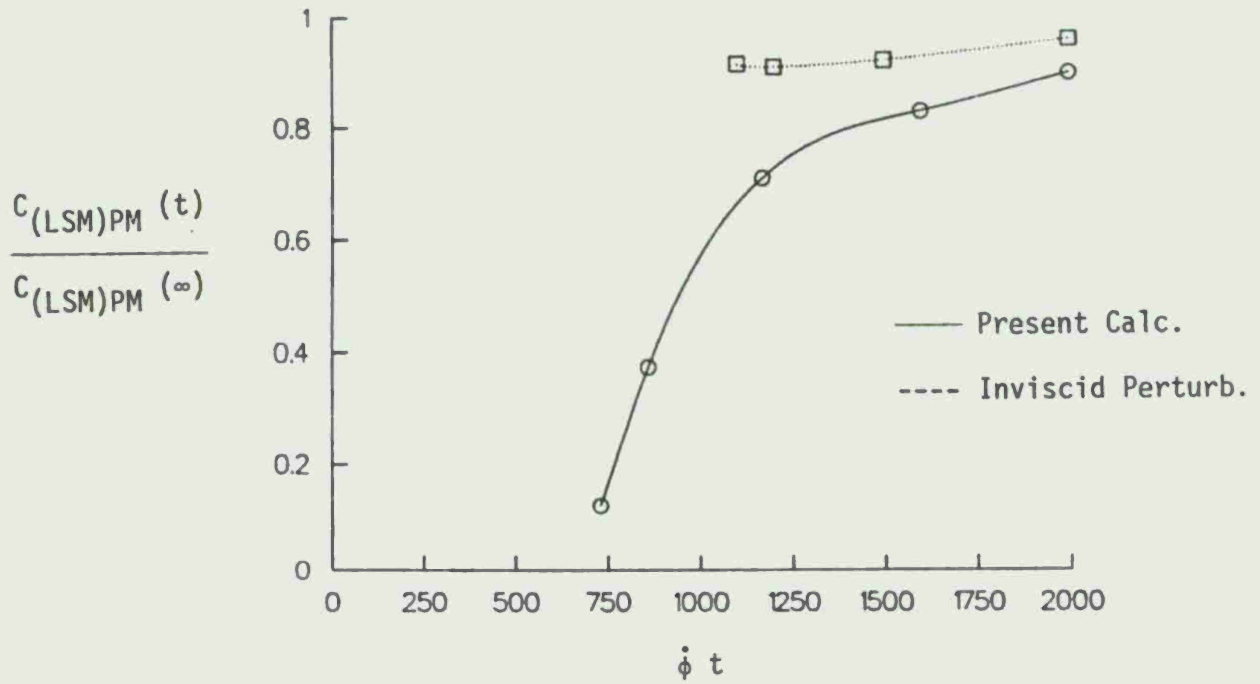

Figure 6. Moment Coefficient Ratio vs $\dot{\phi}$t for Case A: Re = 39772, c/a = 3.12.

REFERENCES

1. C. W. Kitchens, Jr., N. Gerber, and R. Sedney, "Oscilaltions of a Liquid in a Rotating Cylinder: Part I. Solid Body Rotation," BRL Technical Report ARBRL-TR-02081, June 1978. (AD A057759)

2. N. Gerber, R. Sedney, and J. M. Bartos, "Pressure Moment on a Liquid-Filled Projectile: Solid Body Rotation," BRL Technical Report ARBRL-TR-02422, October 1982. (AD A120567)

3. C. H. Murphy, "Angular Motion of a Spinning Projectile with a Viscous Liquid Payload," BRL Memorandum Report ARBRL-MR-03194, August 1982. (AD A118676) (See also Journal of Guidance, Control, and Dynamics, Vol. 6, July-August 1983, pp. 280-286.)

4. N. Gerber and R. Sedney, "Moment on a Liquid-Filled Spinning and Nutating Projectile: Solid Body Rotation," BRL Technical Report ARBRL-TR-02470, February 1983. (AD A125332)

5. K. Stewartson, "On the Stability of a Spinning Top Containing Liquid," Journal of Fluid Mechanics, Vol. 5, Part 4, 1959.

6. E. H. Wedemeyer, "Viscous Corrections to Stewartson's Stability Criterion," BRL Report No. 1287, June 1966. (AD 489687)

7. R. Sedney and N. Gerber, "Oscillations of a Liquid in a Rotating Cylinder: Part II. Spin-Up," BRL Technical Report ARBRL-TR-02489, May 1983. (AD A129094)

8. C. H. Murphy, "Moment Induced by Liquid Payload During Spin-Up Without a Critical Layer," BRL report in preparation. See also AIAA 22nd Aerospace Sciences Meeting, Reno, Nevada, January 1984, AIAA Paper No. 84-0229.

9. H. Schlichting, Boundary Layer Theory, McGraw-Hill Book Co., New York, NY, 1960.

10. E. H. Wedemeyer, "The Unsteady Flow Within a Spinning Cylinder," BRL Report No. 1225, October 1963. (AD 431846). (See also Journal of Fluid Mechanics, Vol. 20, Part 3, 1964, pp. 383-399.)

11. R. Sedney and N. Gerber, "Viscous Effects in the Wedemeyer Model of Spin-Up From Rest," BRL Technical Report ARBRL-TR-02493, June 1983. (AD A129506)

12. R. Sedney and N. Gerber, "Numerical Study of the Critical Layer in a Rotating Fluid," AIAA 22nd Aerospace Sciences Meeting, Reno, Nevada, January 1984, AIAA Paper No. 84-0342.

APPENDIX A

EVALUATION OF VARIABLES ON BOUNDARIES

APPENDIX A: EVALUATION OF VARIABLES ON BOUNDARIES

The relationship between the inertial and nutating sets of cylindrical coordinates is (Eq. (9) in Reference 2)

$$r = \tilde{r} - K_1 \tilde{x} \cos(\tau\dot{\phi}t - \tilde{\theta}) + O(K_o^2) \tag{A.1a}$$

$$\theta = \tilde{\theta} - K_1 (\tilde{x}/\tilde{r}) \sin(\tau\dot{\phi}t - \tilde{\theta}) + O(K_o^2) \tag{A.1b}$$

$$x = \tilde{x} + K_1 \tilde{r} \cos(\tau\dot{\phi}t - \tilde{\theta}) + O(K_o^2) . \tag{A.1c}$$

Recalling Eq. (2.1), velocities are

$$\left.\begin{aligned} u = dr/d\bar{t} = \overset{*}{U} - K_o\overset{*}{u}, \qquad v = r\, d\theta/d\bar{t} = \overset{*}{V} - K_o\overset{*}{v} \\ w = dx/d\bar{t} = \overset{*}{W} - K_o\overset{*}{w} \\ \tilde{u} = d\tilde{r}/d\bar{t}, \qquad \tilde{v} = \tilde{r}\, d\tilde{\theta}/d\bar{t}, \qquad \tilde{w} = d\tilde{x}/d\bar{t}. \end{aligned}\right\} \tag{A.2}$$

The velocity transformation between the earth-fixed and aeroballistic systems is obtained by differentiating Eq. (A.1) with respect to time and substituting the expressions of Eq. (A.2) for the derivatives. Here we make an additional approximation in order to keep the expressions tractable. According to the Wedemeyer model, U and W are both of order $Re^{-1/2}$; we assume the same for $\overset{*}{U}$ and $\overset{*}{W}$. We shall neglect $K_o\, Re^{-1/2}$ and $K_o^2\, Re^{1/2}$ terms in addition to K_o^2 terms. We then obtain for $\varepsilon = 0$, i.e., $K_1 = K_o$,

$$\tilde{u} = \overset{*}{U} - K_o\overset{*}{u} + K_o \times (\overset{*}{V}/r - \tau) \sin(\tau\dot{\phi}t - \theta) \tag{A.3a}$$

$$\tilde{v} = \overset{*}{V} - K_o\overset{*}{v} + K_o \times \tau \cos(\tau\dot{\phi}t - \theta) \tag{A.3b}$$

$$\tilde{w} = \overset{*}{W} - K_o\overset{*}{w} - K_o r (\overset{*}{V}/r - \tau) \sin(\tau\dot{\phi}t - \theta). \tag{A.3c}$$

A variable may be evaluated at $\tilde{r} = 1$ by an expansion about $r = 1$, thus

$$h(\tilde{r} = 1) = h(r = 1) + (\partial h/\partial r)_{r=1} (r_{\tilde{r}=1} - 1) + O(K_o^2).$$

By application of Eq. (A.1a)

$$h\,(\tilde{r} = 1) = h\,(r = 1) - K_o x \cos\,(\tau\dot{\phi}t-\theta)\,(\partial h/\partial r)_{r\,=\,1} + O(K_o{}^2). \qquad (A.4)$$

Equations (A.3) are now evaluated at $\tilde{r} = 1$. Recalling that $\overset{*}{U}$, $\overset{*}{W} = O(Re^{-1/2})$ and $\overset{*}{U}\,(r = 1) = \overset{*}{W}\,(r = 1) = 0$, we apply Eq. (A.4) to Eq. (A.3) to obtain at <u>r = 1</u>:

$$0 = K_o\,[-\overset{*}{u} + x\,(1-\tau)\,\sin\,(\tau\dot{\phi}t-\theta)] + O\,(K_o{}^2,\ Re^{-1/2}\,K_o) \qquad (A.5a)$$

$$1 \cong 1 + K_o\,[-\overset{*}{v} - x\,\{\overset{*}{V}_r(r = 1) - \tau\}\,\cos\,(\tau\dot{\phi}t-\theta)] \qquad (A.5b)$$

$$0 \cong K_o\,[-\overset{*}{w} - (1-\tau)\,\sin\,(\tau\dot{\phi}t-\theta)]. \qquad (A.5c)$$

Finally, replacing $\overset{*}{V}$ in Eq. (A.5b) by V of the Wedemeyer model we obtain the boundary conditions of Eq. (2.6).*

To evaluate P on the endwall, one applies the expansion

$$P\,(\tilde{x} = A,\ \tilde{r}) = P\,(x = A,\ r) + (\tilde{x}_{\tilde{x}\,=\,A} - A)\,(\partial P/\partial x)_{x\,=\,A} + (\tilde{r} - r)\,(\partial P/\partial r)_{r\,=\,r} + O(K_o{}^2). \qquad (A.6)$$

Eqs. (A2), (A4), and (A5) in Reference 2 contain errors. The signs directly following $\overset{*}{\tilde{u}}$, $\overset{*}{\tilde{v}}$, and $\overset{*}{\tilde{w}}$ in the right-hand sides of Eqs. (A2) should all be positive. The minus signs directly following the equals signs in Eqs. (A4) and (A5) should all be changed to plus signs. Also $\overset{*}{v}$ (r = 1) in the last equation of Eqs. (A4) should be replaced by $\overset{*}{w}$ (r = 1).

In the Wedemeyer model $(\partial P/\partial x) = 0$; $(\tilde{r} - r)$ is given by Eq. (A.1a). Thus

$$P(\tilde{r}, \tilde{x} = A) = P(r) + K_0 A (V^2/r) \cos(\tau\dot{\phi}t - \theta) + O(K_0^2). \tag{A.7}$$

The condition of zero normal flow at the endwall is obtained by evaluating Eq. (A.3c) at $x = A$, where $\overset{*}{W} = 0$ and $\overset{*}{V}/r = 1$. The term $\tilde{w}(x = A)$ is zero in our approximation. This is shown in the expansion

$$\tilde{w}(x = A) = \tilde{w}(\tilde{x} = A) + [\tilde{x}(x = A) - A](\partial\tilde{w}/\partial\tilde{x})_{\tilde{x} = A} + O(K_0^2). \tag{A.8}$$

By Eq. (2.5b), $\tilde{w}(\tilde{x} = A) = 0$; by Eq. (A.1c), $[\tilde{x}(x = A) - A] = O(K_0)$; by Eq. (A.3c), $\tilde{w} = \overset{*}{W} + O(K_0)$. In the Wedemeyer model W and its derivatives are of order $Re^{-1/2}$; the same is assumed for $\overset{*}{W}$ and its derivatives. Then $\tilde{w}(x = A) = O(K_0\, Re^{-1/2})$ and is neglected, leaving

$$\overset{*}{w}(x = A) = -(1-\tau)\, r \sin(\tau\dot{\phi}t - \theta), \tag{A.9}$$

and

$$\underline{w}(x = A) = i(1-\tau)\, r. \tag{A.10}$$

APPENDIX B

FORMULAS FOR d_j's IN EQ. (2.17)

APPENDIX B: FORMULAS FOR d_j's IN EQ. (2.17)

We define e_j by

$$e_j \equiv e_{Rj} + i\, e_{Ij} = (\cos \mu_j A + \delta c_E \mu_j \sin \mu_j A)\, d_j \,. \tag{B.1}$$

Eq. (2.31) is now rewritten:

$$F_R + i\, F_I = \psi(r) - \sum_{j=1}^{NJ} [e_{Rj} + i\, e_{Ij}]\, [\bar{w}_{Rj}(r) + i\, \bar{w}_{Ij}(r)], \tag{B.2}$$

where

$$\psi(r) \equiv \psi_R + i\, \psi_I = \hat{w}_o(r) - i\,(1-\tau)\, r \,. \tag{B.3}$$

The boundary condition at $x = A$ is satisfied if $F_R(r)$ and $F_I(r)$ are identically zero. Since they are not, we seek 2 NJ constants, the e_{Rj}'s and e_{Ij}'s that minimize the error defined as

$$g(e_j) \equiv \int_0^1 (F_R^2 + F_I^2)\, dr. \tag{B.4}$$

The minimizing conditions are

$$\partial g/\partial e_{Rj} = 0, \qquad \partial g/\partial e_{Ij} = 0 \qquad j = 1,\ldots,NJ \,. \tag{B.5}$$

Substituting the required terms into Eq. (B.5) and performing the manipulations lead to the linear system for the e_j's ($j = 1,\ldots NJ$):

$$\int_0^1 (\bar{w}_{Rj}\, \psi_R + \bar{w}_{Ij}\, \psi_I)\, dr = \sum_{i=1}^{NJ} e_{Ri} \left[\int_0^1 (\bar{w}_{Rj}\, \bar{w}_{Ri} + \bar{w}_{Ij}\, \bar{w}_{Ii})\, dr\right] + \tag{B.6a}$$

$$\sum_{i=1}^{NJ} e_{Ii} \left[\int_0^1 (-\bar{w}_{Rj}\, \bar{w}_{Ii} + \bar{w}_{Ij}\, \bar{w}_{Ri})\, dr\right]$$

$$\int_0^1 (\bar{w}_{Rj}\ \psi_I - \bar{w}_{Ij}\ \psi_R)\ dr = \sum_{i=1}^{NJ} e_{Ri} \left[\int_0^1 (-\bar{w}_{Ij}\ \bar{w}_{Ri} + \bar{w}_{Rj}\ \bar{w}_{Ii})\ dr\right] +$$

$$\sum_{i=1}^{NJ} e_{Ii} \left[\int_0^1 (\bar{w}_{Ij}\ \bar{w}_{Ii} + \bar{w}_{Rj}\ \bar{w}_{Ri})\ dr\right]. \qquad \text{(B.6b)}$$

The d_j's are then found from Eq. (B.1).

LIST OF SYMBOLS

a	cross-sectional radius of cylinder, Figure 1 [cm]
A	$\equiv c/a$, aspect ratio of cylinder
b_k	biorthogonal coefficients for series of axial eigenfunctions, Eqs. (2.28) and (2.29)
B	function of r defined in Eq. (2.26)
c	half-height of cylinder [cm]
C_R	natural oscillation frequency of rotating liquid/$\dot{\phi}$
$C_{(LM)P}$	complex liquid pressure moment coefficient = $C_{(LSM)P}$ + i $C_{(LIM)P}$, Eq. (3.3)
$C_{(LIM)P}$	pressure in-plane moment coefficient, Eq. (3.18)
$C_{(LSM)P}$	pressure side moment coefficient, Eq. (3.18)
$C_{(LSM)PM}$	maximum value of $C_{(LSM)P}$
d_j	coefficient in series given by the 3rd terms in Eq. (2.17); see also Eq. (2.34)
e_j	coefficient defined in Eq. (B.1)
f	$\equiv (1-i\varepsilon)\tau$, complex representation of angular motion, Eq. (1.4)
F	endwall boundary condition function of r, Eq. (2.31)
I_E	integral occurring in the endwall moment calculation, Eqs. (3.12) and (3.14)
I_S	integral occurring in the sidewall moment calculation, Eqs. (3.8) and (3.10)
j	index in series given by the 3rd terms in Eq. (2.17)
k	index of axial eigenfunction and eigenvalue, Eqs. (2.18) and (2.19)
KF	index of final term of sin $\lambda_k x$ series in Eq. (2.17a)
K_o	yaw amplitude at time t = 0
K_1	$\equiv K_o \; e^{\varepsilon\tau\dot{\phi}t}$, yaw amplitude at time t, Eq. (1.4)
M	$= \tau - V/r$

M_1, M_2	moment terms, Eqs. (3.16) and (3.17)
$M_{(L\tilde{Y})P}$, $M_{(L\tilde{Z})P}$	$\tilde{y}$ and $\tilde{z}$ components, respectively, of liquid moment [g cm^2/s^2]
$M_{(L\tilde{Z}B)P}$, $M_{(L\tilde{Z}T)P}$	bottom and top wall contributions, respectively, to $M_{(L\tilde{Z})P}$ [g cm^2/s^2]
$M_{(L\tilde{Z}E)P}$, $M_{(L\tilde{Z}L)P}$	endwall and sidewall contributions, respectively, to $M_{(L\tilde{Z})P}$ [g cm^2/s^2]
n	index of radial mode for eigenfrequency, C_R
n_{YE}, n_{ZE}	components in the y, z plane of a unit vector lying on the $\tilde{x}$-axis
NJ	number of terms in the series given by the 3rd terms in Eq. (2.17)
p	pressure/$(\rho a^2\dot{\phi}^2)$
$\overset{*}{p}$	perturbation pressure/$(K_0\rho a^2\dot{\phi}^2)$, Eqs. (2.1) and (2.4)
$\overset{*}{p}_c$	complex perturbation pressure/$(K_0\rho a^2\dot{\phi}^2)$, Eq. (2.8)
$\varrho \equiv \varrho_R + i\,\varrho_I$	r,x variation of perturbation pressure/$(K_0\rho a^2\dot{\phi}^2)$, Eq. (2.8d)
$\bar{p}_j(r)$	jth eigenfunction in series given by the 3rd term in Eq. (2.17d)
$\hat{p}_0(r)$	first term in solution to ϱ, Eq. (2.17d)
$\hat{p}_k(r)$	coefficient of kth axial eigenfunction in series given by the 2nd term in Eq. (2.17d)
P	Wedemeyer model approximation to $\overset{*}{P}$ in core flow, Eqs. (2.2b) and (2.2e)
$\overset{*}{P}$	axisymmetric unperturbed pressure/$(\rho a^2\dot{\phi}^2)$, Eq. (2.1d)
P_1	P (r = 1) = constant
r,$\tilde{r}$	(1/a) × radial coordinate in inertial coordinate system and non-rotating aeroballistic system, respectively

Re	Reynolds number = $a^2\dot{\phi}/\nu$
Re_E	"effective" Reynolds number, Eq. (2.14)
t	time [s]
t_M	time at which $C_{(LSM)PM}$ occurs for given τ
$\bar{t}$	$\dot{\phi}t$, non-dimensional time, or total angle of rotation
$u,\tilde{u}$	$(1/[a\dot{\phi}])$ × radial velocity component in inertial frame and non-rotating aeroballistic frame, respectively
$v,\tilde{v}$	$(1/[a\dot{\phi}])$ × azimuthal velocity component in inertial frame and non-rotating aeroballistic frame, respectively
$w,\tilde{w}$	$(1/[a\dot{\phi}])$ × axial velocity component in inertial frame and non-rotating aeroballistic frame, respectively
$\overset{*}{u}$, $\overset{*}{v}$, $\overset{*}{w}$	$(1/[K_o a\dot{\phi}])$ × radial, azimuthal, axial perturbation velocity components in inertial system, Eqs. (2.1) and (2.4)
$\overset{*}{u}_c$, $\overset{*}{v}_c$, $\overset{*}{w}_c$	$(1/[K_o a\dot{\phi}])$ × complex radial, azimuthal, and axial perturbation velocity components, Eq. (2.8)
$\underline{u}$, $\underline{v}$, $\underline{w}$	$(1/[K_o a\dot{\phi}])$ × r,x variation of perturbation velocity components, Eqs. (2.8) and (2.9)
$\hat{u}_o$, $\hat{v}_o$, $\hat{w}_o$	1st terms in right-hand sides of Eqs. (2.17a), (2.17b), and (2.17c)
$\hat{u}_k$, $\hat{v}_k$, $\hat{w}_k$	coefficients of sin $\lambda_k x$ and cos $\lambda_k x$ in series expansions for $\underline{u}$, $\underline{v}$, $\underline{w}$, $\underline{p}$ (2nd terms in Eq. (2.17))
$\bar{u}_j$, $\bar{v}_j$, $\bar{w}_j$	coefficients of sin $\mu_j x$ and cos $\mu_j x$ in series expansions for $\underline{u}$, $\underline{v}$, $\underline{w}$, $\underline{p}$ (3rd terms in Eq. (2.17))
U, V, W	Wedemeyer core flow model approximations to $\overset{*}{U}$, $\overset{*}{V}$, $\overset{*}{W}$
$\overset{*}{U}$, $\overset{*}{V}$, $\overset{*}{W}$	$(1/[a\dot{\phi}])$ × radial, azimuthal, and axial velocity components of unperturbed flow, Eq. (2.1)

LIST OF SYMBOLS (Continued)

x, y, z	rectangular coordinates in inertial system (x-axis along trajectory) [length/a]
$\tilde{x}, \tilde{y}, \tilde{z}$	rectangular coordinates in aeroballistic system ($\tilde{x}$-axis along cylinder axis) [length/a]
$y_1, \ldots, y_6$	functions describing radial variation of perturbation flow variables, Eqs. (2.24) and (2.25)
δc	correction term in endwall boundary condition for solid body rotation
δc_E	correction term in ad hoc endwall boundary condition, Eqs. (2.12) and (2.13)
ε	= $(1/\tau)$ × yaw growth per radian of nutation
ε_p	= 0 for $\lambda_k \neq 0$, = 1 for $\lambda_k = 0$
$\theta, \tilde{\theta}$	polar angles (azimuthal coordinates) in inertial and aeroballistic systems, respectively
λ_k	eigenvalue in the axial problem, Eqs. (2.18) and (2.19)
μ_j	eigenvalues occurring in series given by the 3rd terms in Eq. (2.17); see discussion preceding Eq. (2.20)
ν	kinematic viscosity of liquid [cm^2/s]
$\tilde{\xi}$	vector describing angular motion of cylinder, Eqs. (1.2) and (1.3)
ρ	density of liquid [g/cm^3]
τ	nutational frequency of cylinder/$\dot{\phi}$
τ_M	τ for which $C_{(LSM)PM}$ occurs at a given t
$\dot{\phi}$	spin rate of cylinder [rad/s], taken to be positive
$\psi(r)$	= $\hat{w}_0(r) - i(1 - \tau) r$, Eq. (2.32)

DISTRIBUTION LIST

No. of Copies	Organization
12	Administrator Defense Technical Information Center ATTN: DTIC-DDA Cameron Station Alexandria, VA 22314
1	Director US Army Air Mobility Research and Development Laboratory Ames Research Center Moffett Field, CA 94035
1	Commander US Army Materiel Development and Readiness Command ATTN: DRCDMD-ST 5001 Eisenhower Avenue Alexandria, VA 22333
1	Commander Armament R&D Center US Army AMCCOM ATTN: DRSMC-TDC(D) Dover, NJ 07801
2	Commander Armament R&D Center US Army AMCCOM ATTN: DRSMC-TSS(D) Dover, NJ 07801
5	Commander Armament R&D Center US Army AMCCOM ATTN: DRSMC-LCA-F(D) Mr. D. Mertz Mr. S. Wasserman Mr. A. Loeb Mr. R. Kline Mr. S. Kahn Dover, NJ 07801
1	Commander US Army Engineering Waterways Experiment Station ATTN: R.H. Malter P.O. Box 631 Vicksburg, MS 39180
1	Commander US Army Armament, Munitions and Chemical Command ATTN: DRSMC-LEP-L(R) Rock Island, IL 61299
1	Director Benet Weapons Laboratory Armament R&D Center US Army AMCCOM ATTN: DRSMC-LCB-TL(D) Watervliet, NY 12189
1	Commander US Army Aviation Research and Development Command ATTN: DRDAV-E 4300 Goodfellow Blvd St. Louis, MO 63120
1	Director US Army Air Mobility Research and Development Laboratory ATTN: SAVDL-D, W.J. McCroskey Ames Research Center Moffett Field, CA 94035
1	Commander US Army Communications Research and Development Command ATTN: DRSEL-ATDD Fort Monmouth, NJ 07703
1	Commander US Army Communications Rsch and Development Command ATTN: DRSEL-L Fort Monmouth, NJ 07703
1	Commander US Army Electronics Research and Development Command Technical Support Activity ATTN: DELSD-L Fort Monmouth, NJ 07703

DISTRIBUTION LIST

No. of Copies	Organization
1	Commander US Army Missile Command ATTN: DRSMI-YDL Redstone Arsenal, AL 35898
1	Commander US Army Missile Command ATTN: DRSMI-R Redstone Arsenal, AL 35898
1	Commander US Army Missile Command ATTN: DRSMI-RDK, Mr. R. Deep Redstone Arsenal, AL 35898
1	Commander US Army Tank Automotive Command ATTN: DRSTA-TSL Warren, MI 48090
1	Director US Army TRADOC Systems Analysis Activity ATTN: ATAA-SL White Sands Missile Range, NM 88002
1	Commander US Army Jefferson Proving GD Madison, IN 47251
2	Commander US Army Research Office ATTN: Dr. R.E. Singleton Dr. Jagdish Chandra P.O. Box 12211 Research Triangle Park, NC 27709
1	AGARD-NATO ATTN: R.H. Korkegi APO New York 09777
1	AFWL/SUL Kirtland AFB, NM 87117
2	Commandant US Army Infantry School ATTN: ATSH-CD-CSO-OR Fort Benning, GA 31905
3	Commander Naval Air Systems Command ATTN: AIR-604 Washington, DC 20360
2	Commander David W. Taylor Naval Ship Research & Development Ctr ATTN: H.J. Lugt, Code 1802 S. de los Santos Bethesda, MD 20084
1	Commander Naval Surface Weapons Center ATTN: DX-21, Lib Br Dahlgren, VA 22448
4	Commander Naval Surface Weapons Center Applied Aerodynamics Division ATTN: J.T. Frasier M. Ciment A.E. Winklemann W.C. Ragsdale Silver Spring, MD 20910
1	AFATL (DLDL, Dr. D.C.Daniel) Eglin AFB, FL 32542
1	AFWAL (W. L. Hankey) Wright-Patterson AFB, OH 45433
1	Aerospace Corporation Aero-Engineering Subdivision ATTN: Walter F. Reddall El Segundo, CA 90245
1	AFWAL (J. S. Shang) Wright-Patterson AFB, OH 45433

DISTRIBUTION LIST

No. of Copies	Organization
5	Director National Aeronautics and Space Administration Ames Research Center ATTN: D.R. Chapman J. Rakich W.C. Rose B. Wick P. Kutler Moffett Field, CA 94035
4	Director National Aeronautics and Space Administration Langley Research Center ATTN: E. Price J. South J.R. Sterrett Tech Library Langley Station Hampton, VA 23365
1	Director National Aeronautics and Space Administration Lewis Research Center ATTN: MS 60-3, Tech Lib 21000 Brookpark Road Cleveland, OH 44135
2	Director National Aeronautics and Space Administration Marshall Space Flight Center ATTN: A.R. Felix, Chief S&E-AERO-AE Dr. W.W. Fowlis Huntsville, AL 35812
3	Aerospace Corporation ATTN: H. Mirels R.L. Varwig Aerophysics Lab. P.O. Box 92957 Los Angeles, CA 90009
2	Director Jet Propulsion Laboratory ATTN: L.M. Mach Tech Library 4800 Oak Grove Drive Pasadena, CA 91109
3	Arnold Research Org., Inc. ATTN: J.D. Whitfield R.K. Matthews J.C. Adams Arnold AFB, TN 37389
1	AVCO Systems Division ATTN: B. Reeves 201 Lowell Street Wilmington, MA 01887
3	Boeing Commercial Airplane Company ATTN: R.A. Day, MS 1W-82 P.E. Rubbert, MS 3N-19 J.D. McLean, MS-3N-19 Seattle, WA 98124
3	Calspan Corporation ATTN: G. Homicz P.O. Box 400 Buffalo, NY 14225
1	General Dynamics ATTN: Research Lib 2246 P.O. Box 748 Fort Worth, TX 76101
1	General Electric Company, RESD ATTN: W.J. East 3198 Chestnut Street Philadelphia, PA 19101
2	Grumman Aerospace Corporation ATTN: R.E. Melnik L.G. Kaufman Bethpage, NY 11714

DISTRIBUTION LIST

No. of Copies	Organization
2	Lockheed-Georgia Company ATTN: B.H. Little, Jr. G.A. Pounds Dept 72074, Zone 403 86 South Cobb Drive Marietta, GA 30063
1	Lockheed Missiles and Space Company ATTN: Tech Info Center 3251 Hanover Street Palo Alto, CA 94304
3	Martin-Marietta Corporation ATTN: S.H. Maslen S.C. Traugott H. Obremski 1450 S. Rolling Road Baltimore, MD 21227
2	McDonnell Douglas Astronautics Corporation ATTN: J. Xerikos H. Tang 5301 Bolsa Avenue Huntington Beach, CA 92647
1	Douglas Aircraft Company, Inc. ATTN: T. Cebeci 3855 Lakewood Boulevard Long Beach, CA 90846
3	Rockwell International Science Center ATTN: Dr. V. Shankar Dr. N. Malmuth Dr. S. Chakravarthy 1049 Camino Dos Rios Thousand Oaks, CA 91360
4	Director Sandia National Laboratory ATTN: H.W. Vaughn F.G. Blottner W.L. Oberkampf Tech Library Albuquerque, NM 87115
2	United Aircraft Corporation Research Laboratory ATTN: M.J. Werle; Library 400 Main Street East Hartford, CT 06108
1	LTV Aerospace Corporation Vought Systems Division ATTN: J.M. Cooksey, Chief, Gas Dynamics Lab, 2-53700 P.O. Box 5907 Dallas, TX 75222
1	Arizona State University Department of Mechanical and Energy Systems Engineering ATTN: G.P. Neitzel Tempe, AZ 85281
1	Cornell University Graduate School of Aero Engr ATTN: Library Ithaca, NY 14850
3	California Institute of Technology ATTN: Tech Library H.B. Keller, Math Dept D. Coles, Aero Dept Pasadena, CA 91109
1	Illinois Institute of Technology ATTN: H. M. Nagib 3300 South Federal Chicago, IL 60616
1	The Johns Hopkins University Dept of Mech and Materials Sci. ATTN: S. Corrsin Baltimore, MD 21218

DISTRIBUTION LIST

No. of Copies	Organization
4	Director Johns Hopkins University Applied Physics Laboratory ATTN: Dr. R.D. Whiting Dr. D.A. Hurdif Dr. R.S. Hirsh Mr. E.R. Bohn Johns Hopkins Road Laurel, MD 20707
3	Massachusetts Institute of Technology ATTN: E. Covert H. Greenspan Tech Lib 77 Massachusetts Avenue Cambridge, MA 02139
2	North Carolina State Univ Mechanical and Aerospace Engineering Department ATTN: F.F. DeJarnette J.C. Williams Raleigh, NC 27607
1	Northwestern University Department of Engineering Science and Applied Mathematics ATTN: Dr. S.H. Davis Evanston, IL 60201
1	Notre Dame University Department of Aero Engr ATTN: T.J. Mueller Notre Dame, IN 46556
2	Ohio State University Dept of Aeronautical and Astronautical Engineering ATTN: S.L. Petrie O.R. Burggraf Columbus, OH 43210
2	Polytechnic Institute of New York ATTN: G. Moretti S.G. Rubin Route 110 Farmingdale, NY 11735
3	Director Forrestal Research Ctr Gas Dynamics Laboratory Princeton University ATTN: S.M. Bogdonoff; S.I. Cheng Tech Library Princeton, NJ 08540
1	Purdue University Thermal Science & Prop Ctr ATTN: Tech Library W. Lafayette, IN 47906
1	Rensselaer Polytechnic Institute Department of Math Sciences ATTN: R.C. Di Prima Troy, NY 12181
1	Southern Methodist University Dept. of Civil and Mechanical Engineering ATTN: R. L. Simpson Dallas, TX 75222
1	San Diego State University Department of Aerospace Engr and Engineering Mechanics College of Engineering ATTN: K.C. Wang San Diego, CA 92115

DISTRIBUTION LIST

No. of Copies	Organization
1	Southwest Research Institute Applied Mechanics Reviews 8500 Culebra Road San Antonio, TX 78228
2	Stanford University Dept of Aeronautics/Astronautics ATTN: Dr. J.L. Steger Dr. S. Chakravarthy Stanford, CA 94305
1	Texas A&M University College of Engineering ATTN: R.H. Page College Station, TX 77843
1	University of California - Davis ATTN: H.A. Dwyer Davis, CA 95616
1	University of California - Berkeley Department of Aerospace Engineering ATTN: M. Holt Berkeley, CA 94720
2	University of California - San Diego Department of Aerospace Engineering and Mechanical Engineering Sciences ATTN: P. Libby Tech Library La Jolla, CA 92093
1	University of Cincinnati Department of Aerospace Engineering ATTN: R.T. Davis Cincinnati, OH 45221
1	University of Colorado Department of Astro-Geophysics ATTN: E.R. Benton Boulder, CO 80302
2	University of Maryland ATTN: W. Melnik J.D. Anderson College Park, MD 20740
1	University of Maryland - Baltimore County Department of Mathematics ATTN: Dr. Y.M. Lynn 5401 Wilkens Avenue Baltimore, MD 21228
1	University of Santa Clara Department of Physics ATTN: R. Greeley Santa Clara, CA 95053
2	University of Southern California Department of Aerospace Engineering ATTN: T. Maxworthy P. Weidman Los Angeles, CA 90007
2	University of Michigan Department of Aeronautical Engineering ATTN: W.W. Wilmarth Tech Library East Engineering Building Ann Arbor, MI 48104
2	University of Rochester Department of Mechanical and Aerospace Sciences ATTN: R. Gans A. Clark, Jr. Rochester, NY 14627
1	University of Tennessee Department of Physics ATTN: Prof. W.E. Scott Knoxville, TN 37916

DISTRIBUTION LIST

No. of Copies	Organization
1	University of Texas Department of Aerospace Engineering ATTN: J.C. Westkaemper Austin, TX 78712
1	University of Virginia Department of Aerospace Engineering & Engineering Physics ATTN: I.D. Jacobson Charlottesville, VA 22904
1	University of Virginia Research Laboratories for the Engineering Sciences ATTN: Prof. H. G. Wood P.O. Box 3366 University Station Charlottesville, VA 22903
1	University of Washington Department of Mechanical Engineering ATTN: Tech Library Seattle, WA 98105
1	University of Wyoming ATTN: D.L. Boyer University Station Laramie, WY 82071
1	U.S. Military Academy Department of Physics ATTN: MAJ G. Heuser West Point, NY 10996
1	Woods Hole Oceanographic Institute ATTN: J.A. Whitehead Woods Hole, MA 02543
3	Virginia Polytechnic Institute and State University Department of Aerospace Engineering ATTN: Tech Library Dr. W. Saric Dr. T. Herbert Blacksburg, VA 24061

Aberdeen Proving Ground

Director, USAMSAA
ATTN: DRXSY-D
DRXSY-MP, H. Cohen

Commander, USATECOM
ATTN: DRSTE-TO-F

Commander, CRDC, AMCCOM
ATTN: DRSMC-CLN
W. C. Dee
DRSMC-CLB-PA
M. C. Miller
DRSMC-CLJ-L
DRSMC-CLB-PA
DRSMC-CLN

USER EVALUATION OF REPORT

Please take a few minutes to answer the questions below; tear out this sheet, fold as indicated, staple or tape closed, and place in the mail. Your comments will provide us with information for improving future reports.

1. BRL Report Number _____

2. Does this report satisfy a need? (Comment on purpose, related project, or other area of interest for which report will be used.)

_____

_____

_____

3. How, specifically, is the report being used? (Information source, design data or procedure, management procedure, source of ideas, etc.) _____

_____

_____

4. Has the information in this report led to any quantitative savings as far as man-hours/contract dollars saved, operating costs avoided, efficiencies achieved, etc.? If so, please elaborate.

_____

_____

5. General Comments (Indicate what you think should be changed to make this report and future reports of this type more responsive to your needs, more usable, improve readability, etc.) _____

_____

_____

_____

6. If you would like to be contacted by the personnel who prepared this report to raise specific questions or discuss the topic, please fill in the following information.

Name: _____

Telephone Number: _____

Organization Address: _____

_____

_____